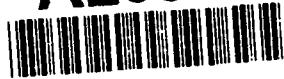


AD-A269 450



WL-TR-93-2083



**STUDIES ON GEL ELECTROLYTE BASED ON
NITRILE-BUTADIENE COPOLYMERS**

A. K. Sircar, B. Kumar, S. M. Linden, and P.T. Weissman

University of Dayton Research Institute
300 College Park Avenue
Dayton, Ohio 45469-0130

June 1993



Final Report for Period November 1991 - November 1992

Approved for public release; distribution is unlimited.

AERO PROPULSION & POWER DIRECTORATE
WRIGHT LABORATORY
AIR FORCE MATERIEL COMMAND
WRIGHT-PATTERSON AIR FORCE BASE, OHIO 45433-7650

93-21625



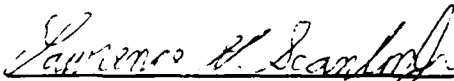
ENP X

NOTICE

When Government drawings, specifications, or other data are used for any purpose other than in connection with a definitely Government-related procurement, the United States Government incurs no responsibility or any obligation whatsoever. The fact that the government may have formulated or in any way supplied the said drawings, specifications, or other data, is not to be regarded by implication, or otherwise in any manner construed, as licensing the holder, or any other person or corporation; or as conveying any rights or permission to manufacture, use, or sell any patented invention that may in any way be related thereto.

This report is releasable to the National Technical Information Service (NTIS). At NTIS, it will be available to the general public, including foreign nations.

This technical report has been reviewed and is approved for publication.



DR. LAWRENCE G. SCANLON, JR.
Project Scientist



MR. RICHARD A. MARSH, Chief
Battery Electrochemistry Section
Power Technology branch



MICHAEL D. BRAYDICH, Lt Col, USAF
Deputy Director
Aerospace Power Division
Aero Propulsion & Power Directorate

If your address has changed, if you wish to be removed from our mailing list, or if the addressee is no longer employed by your organization, please notify WL/POOS, WPAFB, OH 45433-7251 to help us maintain a current mailing list.

Copies of this report should not be returned unless return is required by security considerations, contractual obligations, or notice on a specific document.

REPORT DOCUMENTATION PAGE			Form Approved OMB No. 0704-0188	
<small>Public reporting burden for this collection of information is estimated to average 1 hour per response, including the time for reviewing instructions, searching existing data sources, gathering and maintaining the data needed, and completing and reviewing the collection of information. Send comments regarding this burden estimate or any other aspect of this collection of information, including suggestions for reducing this burden, to Washington Headquarters Services, Directorate for Information Operations and Reports, 1215 Jefferson Davis Highway, Suite 1204, Arlington, VA 22202-4302, and to the Office of Management and Budget, Paperwork Reduction Project (0704-0188), Washington, DC 20503.</small>				
1. AGENCY USE ONLY (Leave blank)		2. REPORT DATE Jun 1993	3. REPORT TYPE AND DATES COVERED 1 November 1991 - 30 November 1992	
4. TITLE AND SUBTITLE Studies on Gel Electrolyte Based on Nitrile-Butadiene Copolymers			5. FUNDING NUMBERS C - F33615-90-C-2036 PE - 62203 PR - 3145 TA - 32 WU - 20	
6. AUTHOR(S) A.K. Sircar, B. Kumar, S.M. Linden, P.T. Weissman				
7. PERFORMING ORGANIZATION NAME(S) AND ADDRESS(ES) University of Dayton Research Institute 300 College Park Ave Dayton OH 45469-0130			8. PERFORMING ORGANIZATION REPORT NUMBER	
9. SPONSORING / MONITORING AGENCY NAME(S) AND ADDRESS(ES) Aero Propulsion & Power Directorate Wright Laboratory Air Force Materiel Command Wright-Patterson AFB OH 45433-7650			10. SPONSORING / MONITORING AGENCY REPORT NUMBER WL-TR-93-2083	
11. SUPPLEMENTARY NOTES				
12a. DISTRIBUTION / AVAILABILITY STATEMENT Approved for Public Release; Distribution is unlimited			12b. DISTRIBUTION CODE	
13. ABSTRACT (Maximum 200 words) This study is concerned with the preparation of a hybrid electrolyte, suitable for solid-polymer batteries. Based on the study of ionic conductivity in the presence of LiBF_4 of a number of nitrile-butadiene copolymers (NBR), hydrogenated NBR (HNBR) was selected as the host polymer. DC conductivity studies with three different lithium salts in different plasticizers showed the highest conductivity for LiBF_4 . Conductivity of LiBF_4 in different plasticizers decreases in the order $\text{DMF} > \text{DMAC} > \gamma\text{-butyrolactone} > \text{NMP} > \text{PC} = \gamma\text{-valerolactone} > \text{glymes}$. NMP was chosen as the plasticizer for hybrid films based on its moderate conductivity, low vapor pressure, and low freezing point.				
14. SUBJECT TERMS Polymer electrolytes, Gel electrolytes, ionic conductivity			15. NUMBER OF PAGES 82	
			16. PRICE CODE	
17. SECURITY CLASSIFICATION OF REPORT UNCLASSIFIED	18. SECURITY CLASSIFICATION OF THIS PAGE UNCLASSIFIED	19. SECURITY CLASSIFICATION OF ABSTRACT UNCLASSIFIED	20. LIMITATION OF ABSTRACT UL	

CONTENTS

<u>SECTION</u>	<u>PAGE</u>
FIGURES	iii
TABLES	vi
ACKNOWLEDGMENTS	vii
1 INTRODUCTION	1
2 BACKGROUND	1
3 EXPERIMENTAL	3
Polymers.....	3
Plasticizers.....	3
Inorganic Salts.....	3
Synthesis of Gel Electrolytes and Films.....	3
Thermogravimetry	5
Infrared Spectroscopy	5
Impedance Spectroscopy.....	7
Conductivity Measurements.....	7
Cyclic Voltametry.....	8
4 RESULTS AND DISCUSSIONS	9
Selection of Host Polymer	9
Specific Conductivity of Inorganic Salts in Different Organic Plasticizers	9
Selection of the NBR Copolymer.....	20
Specific Conductivity of Gel Electrolyte by DC Conductivity	23
Conductivity of Hybrid Films by Impedance Measurement	27
Thermogravimetric Analysis of Gel Electrolyte.....	33
IR Studies of Gel Electrolyte	36
Cyclic Voltammetry.....	45
5 SUMMARY AND CONCLUSIONS	48
6 RECOMMENDATIONS	48
REFERENCES	49

CONTENTS (Continued)

SECTION	PAGE
APPENDIX A: GLASS TRANSITION TEMPERATURE OF VARIOUS NBR COPOLYMERS WITH AND WITHOUT LiBF_4	53
APPENDIX B: ANOMALY IN THE IONIC CONDUCTIVITY-TEMPERATURE STUDIES OF NBR COPOLYMERS USING DEA	63

Accession For		
NTIS	GR131	V
DIE	102	U
U. S. Navy		U
Justification		
By		
Distribution		
Availability		
Dist	Availability	Special
A-1		

DTIC QUALITY INSPECTED 4

FIGURES

FIGURE		PAGE
1	Setup for Conductivity Measurements by Impedance.....	6
2	Conductivity of Aqueous Potassium Chloride Solution at Different Temperature for Calibration of Cell Constant.....	8
3	Chemical Formulae of the Plasticizers Used.....	10
4	Conductivity of LiBF_4 in Different Plasticizers.....	14
5	Conductivity of LiAsF_6 in Different Plasticizers.....	14
6	Conductivity of LiCF_3SO_3 in Different Plasticizers.....	15
7	Conductivity of LiBF_4 in 2-Methoxyethyl Ether.....	17
8	Conductivity of Different Lithium Salts in NMP.....	21
9	Conductivity of LiBF_4 vs Concentration in Different Plasticizers.....	21
10	Conductivity vs Molar Ratio of HNBR/ LiBF_4 in NMP at Various Temperatures.....	24
11	Arrhenius Plot of Log Conductivity vs $1/T$ (K) of Different Concentrations of LiBF_4 in NMP.....	24
12	Arrhenius Plot of Log Conductivity vs $1/T$ (K) of HNBR/ LiBF_4 (CN/Li=8) in Different Solvents.....	26
13	Arrhenius Plot of Log Conductivity vs $1/T$ (K) LiBF_4 in NMP With and Without HNBR.....	26
14	Arrhenius Plot of Log Conductivity vs $1/T$ (K) for Different Ratios of Polymer/Lithium in NMP.....	27
15	Conductivity of Hybrid Films by Complex Impedance Measurement.....	30
16	Conductivity of Hybrid Films vs Time by Impedance Measurement.....	30
17	Conductivity as a Function of CN/Li Ratio and Plasticizer Concentration.....	31
18	Arrhenius Plot of Log Conductivity vs $1/T$ (K) for the Hybrid Film CN/Li/NMP=8/1/13.....	33
19	TG-DTG Curve of HNBR (milled).....	34

LIST OF FIGURES (Continued)

FIGURE		PAGE
20	TG-DTG Curve of NMP	34
21	TG-DTG Curve of LiBF ₄	35
22	TG-DTG Curve of HNBR/LiBF ₄ (15.64/6.16/78.2).	35
23	TG-DTG Curve of HNBR/LiBF ₄ (65/35) Solids Weighed Directly into the TG Pan	37
24	TG-DTG Curve of HNBR/LiBF ₄ (CN/Li=2) Cast From a DMF Solution and Dried in a Vacuum Dessicator for 3 Days..	37
25	IR Absorbance Spectra for A) HNBR With LiBF ₄ (CN/Li=4) and B) HNBR Alone	39
26	IR Transmission Spectra of A) NBR (44% ACN) with LiBF ₄ (CN/Li=2) and B) NBR Alone. Both cast from DMF Solution	39
27	IR Absorbance Spectra of A) NBR (28% ACN) with LiBF ₄ (CN/Li=2) and B) NBR (28% ACN) Alone.....	40
28	IR Absorbtion Ratio (2262/2236 cm ⁻¹ vibrations) vs Percent Li in Li/NBR Film	41
29	IR Absorbance Spectra of A) HNBR/LiBF ₄ /NMP Gel (CN/Li=4) and B) NMP	41
30	IR Absorbance Spectra of A) HNBR Film from NMP and B) HNBR Film from DMF.....	42
31	IR Absorbance Spectra of A) NMP and B) LiBF ₄ , Cast from NMP Solution	42
32	IR Absorbance Spectra of A) NMP and B) PAN/LiBF ₄ (CN/Li=4) Film from a 3% NMP Solution.....	43
33	IR Absorbance Spectra of A) PAN in a KBV Plate and B) PAN/LiBF ₄ (CN/Li=4) Film, Cast from a 3% NMP Solution and Dried for 5 Days in the IR Compartment	44
34	IR Absorbance Spectra of A) PAN Film, Cast from a DMF Solution and Dried for 2 Days and B) PAN/LiBF ₄ (CN/Li=4) Film, Cast from a 3% DMF Solution and Dried for 3.5 Days ..	44

LIST OF FIGURES (Continued)

FIGURE		PAGE
35	IR Absorbance Spectra of A) NBR (44% ACN), Cast from DMF Solution and B) NBR (44% ACN/LiBF ₄ , Cast from a 5% DMF Solution and Dried 10 Days in IR Compartment.....	46
36	Cyclic Voltammogram for 10% LiBF ₄ in NMP with a Lithium Working Electrode and a Lithium Reference Electrode (20 mV/s, ± 3.00 Vdc.....	47
A-1	Glass Transition Temperature of NBR Copolymer (Nipol 1000X88) with 44% ACN.....	56
A-2	Glass Transition Temperature of NBR Copolymer (Nipol 1034-60) with 20% ACN.....	56
A-3	Relationship Between ΔT_g Versus Percent ACN in NBR Copolymers.....	58
A-4	DSC T_g of NBR Copolymer (Nipol 1042) with 35% ACN.....	58
B-1	DEA Curves of Hydrogenated HNBR (44% ACN, Zetpol 1020) Films Prepared from DMF Solutions.....	65
B-2	Expanded DEA Curve of HNBR (44% ACN, Zetpol 1020). A=1st heat, B=2nd heat, C=cooling.....	65
B-3	Expanded DEA Curve of HNBR 44/LiBF ₄ (CN/Li=8). A=1st heat, B=2nd heat, C=cooling.....	67
B-4	DEA Curve of Polyacrylonitrile (PAN Dried from DMF).....	67
B-5	DEA Curve of PAN/LiBF ₄ (CN/Li=8). A=1st heat, B=2nd heat, C=cooling.....	68
B-6	DEA Curve for PEO.....	68
B-7	DEA Curve for PEO After 68 Hours at 43% Relative Humidity.....	69
B-8	T_g Determinant of NBR (28.3% ACN, Nipol 1453). Note the small endotherm after the T_g Region.....	69
B-9	DEA Curve of PAN/LiBF ₄ /EC (CN/Li=4, 25% EC).....	72
B-10	DEA Curve of Zetpol 1020/LiBF ₄ /DMAC (CN/Li=8, 75% DMAC) Gel.....	72

TABLES

TABLE		PAGE
1	Composition of Polymer Solutions and Films.....	4
2	Summary of Conductivity Data (1-5% LiBF ₄) in Different Plasticizers	12
3	Summary of Conductivity Data (1-5% LiAsF ₆) in Different Plasticizers	13
4	Summary of Conductivity Data (1-5% LiCF ₃ SO ₃) in Different Plasticizers	13
5	Melting and Boiling Points of Different Plasticizers.....	16
6	Physical Data for Some Plasticizers and Host Materials	18
7	Summary of Conductivity Data of Two-Plasticizer System (50:50) with 3% LiBF ₄	19
8	Solubility of NBR Copolymer in Different Solvents.....	22
9	Conductivity of NBR and HNBR Elastomers with LiBF ₄ (CN:Li=8) at Various Temperatures at 10 ⁵ Hz	22
10	Composition vs Ionic Conductivity of Hybrid Films	28
A-1	Glass Transition Temperature of NBR Copolymers.....	55
A-2	Glass Transition Temperatures of Various NBR Copolymers With or Without Lithium Tetrafluoroborate	60
B-1	NBR (or HNBR) Copolymers Used for the Study Versus Percent Bound ACN.....	64
B-2	Conductivity of NBR and HNBR Elastomers with LiBF ₄ (CN:Li=8) at Different Temperatures at 10 ⁵ Hz	73

ACKNOWLEDGMENTS

The authors would like to thank Dick Marsh for valuable comments and Dr. Larry Scanlon for helpful criticism during the course of this investigation. Thanks are also due to Mary Galaska and Jeff Schaffer for the solution conductivity data and other experimental help. Niki Maxwell's contribution in compiling this report is gratefully acknowledged. This work was funded by the Aero Propulsion & Power Directorate of Wright Laboratory, Wright-Patterson Air Force Base under Contract No. F33615-90-C-2036.

1. INTRODUCTION

The development of polymeric electrolytes with a room temperature conductivity of 10^{-3} S/cm desirable for solid state rechargeable lithium batteries still remains an elusive goal. Several discoveries in the past few years such as synthesis of poly[bis-(methoxyethoxyethoxide) phosphazene] (MEEP)^[1] and lithium bis (trifluoro methanesulfone) imide, $\text{LiN}(\text{CF}_3\text{SO}_2)_2$,^[2] have been successful in closing the conductivity gap from 10^{-8} S/cm to the 5×10^{-5} S/cm range for (PEO:LiX) film. Further increase of conductivity in a dimensionally stable polymeric electrolyte consisting of an ionizable lithium salt in a polymeric host materials remains a goal. This is understandable in view of the accepted theory of the mechanism of the ion transport via the large-amplitude segmental motion of the amorphous chains of the polymer backbone.^[3]

A promising approach to increase the conductivity of polymeric electrolyte is through the use of low molecular weight organic solvents as plasticizers in a host polymer. This approach uses the smaller activation barrier for conducting ions in the plasticizer phase than in a polymer. In addition, the low viscosity and high dielectric constant of these plasticizers ensures higher mobility and greater dissociation of ion pairs. The polymeric electrolytes obtained by combining a host polymer with a non-aqueous organic liquid containing the ionizable lithium salt are variously known as "Gel Electrolytes" or "Hybrid Electrolytes." These new materials have stimulated major research and development efforts in polymer electrolyte battery technology.

The present work endeavors to use the gel electrolyte concept to prepare 'free standing' films of a nitrile-butadiene copolymer as host material and selected organic solvents as plasticizers. Ionic conductivity was measured as a function of temperature to determine the energy of activation for ion transport. This was carried out for the solution of the electrolyte in the selected plasticizer, with or without the polymer, as well as in the semi-solid hybrid film containing all components. These experiments enable us to delineate the role of the plasticizer versus the host polymer in the gel electrolyte system.

2. BACKGROUND

In recent years attempts have been made to utilize the concept of "Gel Electrolytes" to improve the room temperature conductivity of polyethylene oxide. The plasticizers used are polyethylene glycol dimethyl ether^[3] (PEGDME), propylene carbonate^[4,5] (PC), polyethylene glycol (PEG), and ethylene glycol dimethyl ether (EGDME)^[6]. Plasticizing with PEGDME produced a polymer electrolyte with conductivity in the region 10^{-3} S/cm at

around 40°C, which should be adequate for some applications. The addition of PC resulted in similar conductivity at room temperature. Other polymers and plasticizer have also been used with some success [7-22].

It should be mentioned that PEO dissolves in PC, so the dimensional stability of films containing such miscible components is not satisfactory. On the other hand, if the polymer solvent pair is completely immiscible, the polymer will not swell and the solvent will remain as a separate phase, thus inhibiting its incorporation into the film. The aim should therefore be to obtain a partially miscible polymer-solvent combination, so the polymer can be swollen in the solvent and high conductivity can be obtained in a dimensionally stable film.

Apart from PEO, other polymers used as hosts are polyacrylonitrile (PAN)^[5,18,21], polyvinyl carbonate (PVCa), poly(vinyl pyrrolidone) (PVP)^[17], and poly(vinylidene fluoride) (PVdF). Polystyrene, poly(vinyl chloride) (PVC), and poly(vinyl alcohol) (PVA) have also been used without success, since these polymers do not give a homogeneous molecular dispersion of either LiClO₄ or the plasticizers. The ionic conductivity shows no relationship to the glass transition temperature (T_g) of the polymers.

Plasticizers other than those mentioned above that have been tried are: dimethyl formamide (DMF), dimethyl acetamide (DMAC), γ -butyrolactone (BL), γ -valerolactone (VL), ethylene carbonate (EC), 1,2-dimethoxyethane (DME), dioxolane (DOL), methyl formate (MF) and sulfolane. Electrolyte salts used are LiClO₄, LiCF₃SO₃ and LiAsF₆. The group at Hydro-Quebec has published performance data on primary and secondary batteries^[16]; however, the nature of the electrolyte was not disclosed. Similar data have been published by the Harwell group^[23].

More recently, Lundsguard et al.^[24] reported a polymer electrolyte composition which combines a conductivity greater than 10⁻³ S/cm at room temperature with desirable mechanical properties. Efforts are being made for scaleup and commercialization of this technology^[25]. A gel electrolyte with a room temperature conductivity of the order of 10⁻³ S/cm⁻¹ and a lithium transport number of 0.7 was composed of 2-acrylamido 2-methyl propane sulfonate, lithium carbonate, and lithium trifluoromethane sulfonate salt as dopant^[26].

As would be expected, the mechanical strength of the hybrid films is not as good as the films without the solvent. Abraham and Alamgir^[27] proposed the minimum requirement for these films. It should be possible to process the polymer electrolyte into a free standing

film which can withstand the physical abuse during cell fabrication and cycling of secondary lithium batteries. The strength requirement of these films should possibly be comparable to porous polyethylene and polypropylene membranes of typical thicknesses of 0.0025 to 0.005 cm, used as battery separators for aqueous liquid electrolyte batteries. In addition, Abraham and Alamgir^[27] considers the coexistence of ionic conductivity similar to liquid electrolytes with mechanical properties similar to the unplasticized polymer to be mutually exclusive.

3. EXPERIMENTAL

Polymers. The nitrile butadiene copolymers (NBR) used were commercial elastomers obtained from Zeon Chemical Corporation. They are copolymers of acrylonitrile and butadiene, with the approximate bound acrylonitrile given in parenthesis. Nipol 1000X132 (50.5), Nipol 1000X88 (43.9), Nipol 1401LG (40.9), Nipol 1042 (35), Nipol 1453HM (28.3), Nipol 1034-60 (20.3), Zetpol 1020 (44.5) and Polyacrylonitrile (100). Zetpol 1020 is a hydrogenated NBR (HNBR) with about the same amount of acrylonitrile as Nipol 1000X88. The polymers were used as such after vacuum drying at 60°C for 24 hours.

Plasticizers. The plasticizers used were mono-EGDME, diEGDME, triEGDME, tetraEGDME, BL, VL, N-methyl pyrrolidinone (NMP), DMF, DMAC, and PC. All plasticizers were dried with *molecular sieves*. In addition, NMP used for making films was passed through an activated alumina column in a dry box.

Inorganic Salts. Inorganic salts used as electrolytes were lithium tetrafluoroborate (LiBF_4), lithium hexafluoroarsenate (LiAsF_6) and lithium trifluoromethane sulfonate (LiCF_3SO_3). Samples were opened and used only in the dry box, except for dielectric analysis and infrared studies. In the latter case, they were stored in a dessicator.

Synthesis of Gel Electrolytes and Films. A small magnetic stirring bar was placed in a 50 mL round-bottom wide-mouth flask, and the appropriate amounts of LiBF_4 , Zetpol 1020, and NMP were weighed in (see Table 1). The flask was covered with Parafilm and heated to 120°C while stirring until a solution was obtained (a minimum of 4 hours, but typically overnight). Depending on the concentration of NMP, the solution turns into a gel when cooled to room temperature.

TABLE 1

COMPOSITION OF POLYMER SOLUTIONS AND FILMS

A. SOLUTIONS

Solutions	CN:Li	Wt LiBF ₄ (g)	Wt Zetpol (g)	Wt Solvent
LiBF ₄ in NMP (~2.5%)	2:1	0.200	---	7.650
Zetpol 1010/LiBF ₄ in NMP	2:1	(1) 0.200 (2) 0.200	(1) 0.508 (2) 0.508	(1) 7.632 (2) 7.636
Zetpol 1020/LiBF ₄ in NMP	4:1	0.200	1.016	15.252
Zetpol 1020/LiBF ₄ in NMP	8:1	0.200	2.033	30.502
Zetpol 1020/LiBF ₄ in DMAC	8:1	0.200	2.033	30.508
Zetpol 1020/LiBF ₄ in B-lactone	8:1	0.200	2.033	30.493

B. FILMS

C N:Li	NMP/ Z-1020	Weight (grams)			% Before Pressing			% LiBF ₄ in NMP	Comments
		Z-1020	NMP	LiBF ₄	Z-1020	NMP	LiBF ₄		
1.97	3.03	2.476	7.51	0.988	22.6	68.4	9	13.16	
3.01	3.01	2.501	7.527	0.654	23.4	70.5	6.1	8.69	
3.99	3	2.501	7.512	0.493	23.8	71.5	4.7	6.56	Visc Liq
6.26	2.93	2.554	7.495	0.321	24.6	72.3	3.1	4.28	Visc Liq
8.09	3.02	2.488	7.507	0.242	24.3	73.3	2.4	3.22	Visc Liq
4.02	1.99	3.015	6.01	0.591	31.4	62.5	6.1	9.83	Too soft
4.03	2.23	3.027	6.751	0.591	29.2	65.1	5.7	8.75	Too soft
3.97	1.78	3.002	5.35	0.595	33.6	59.8	6.7	11.12	
4	1.5	3	4.5	0.591	37.1	55.6	7.3	13.13	
2.05	1.93	3.065	5.906	1.179	30.2	58.2	11.6	19.96	No solvate
3	1.77	2.993	5.307	0.784	32.9	58.4	8.6	14.77	
8.11	1.49	3.019	4.498	0.293	38.7	57.6	3.8	6.51	No free film
16.03	1.5	2.994	4.498	0.147	39.2	58.9	1.9	3.27	

The CN:Li ratio influenced the properties of the films. The compositions which contain CN:Li ratios of 2 and 3 are gels at room temperature with NMP:CN=3 and, while soft can be cut with a knife. Those with higher CN:Li ratios are softer and need lower NMP in order to obtain a free-standing film.

The film fabrication technique consisted of weighing 0.7 gm of the gel, sandwiching the gel between two nonporous Teflon sheets, and applying a pressure of 100 lb through two steel plates for approximately 15 minutes. The polymer film was carefully removed from the Teflon sheets without stretching. The films were reweighed to determine any loss of solvent.

The above procedure was used for the gel containing CN:Li=4 having NMP:Z-1020=1.5 and the gel containing CN:Li=3 with NMP:Z-1020=1.75. The procedure was modified by reducing the press load to 50 lb and the time in the press shortened to 1 minute for the gel containing CN:Li=4 with NMP:Z-1020=1.75.

The gel containing CN:Li=8 with NMP:Z-1020=1.5 was too sticky to press between the teflon film as it would split when attempting to remove it. In order to measure the conductivity of those materials which were too sticky to form a free standing film, a different procedure was used. These materials were characterized by presetting the gap between the parallel plates to 0.0381 cm in the conductivity apparatus shown in Figure 1. With the top plate in the raised position, approximately 0.7 gm of the sample was placed in the center of the lower plate. The top plate was then lowered onto the sample and it was "Squeezed" down to the preset thickness. For these materials the polymer electrolyte film thickness is assumed to be the same as the preset distance between the parallel plates.

Thermogravimetry. TA Instruments 2950 Thermogravimetric Analyzer (TGA), calibrated at the melting temperature of indium (156.6°C) was used. Samples were run at 10°C/min under nitrogen or air as appropriate.

Infrared Spectroscopy. Infrared (IR) vibrational spectra were obtained using a Nicolet SX60 FTIR spectrometer.

For infrared measurements, three or four drops of the solutions containing the polymer and the inorganic salt in desired proportion were placed on a sodium chloride plate. The films were dried either inside the IR compartment by passing dry air overnight or under 10 inches vacuum for 1 hour at 50°C. Some samples were subsequently vacuum dried for 24 hours at 80°C.

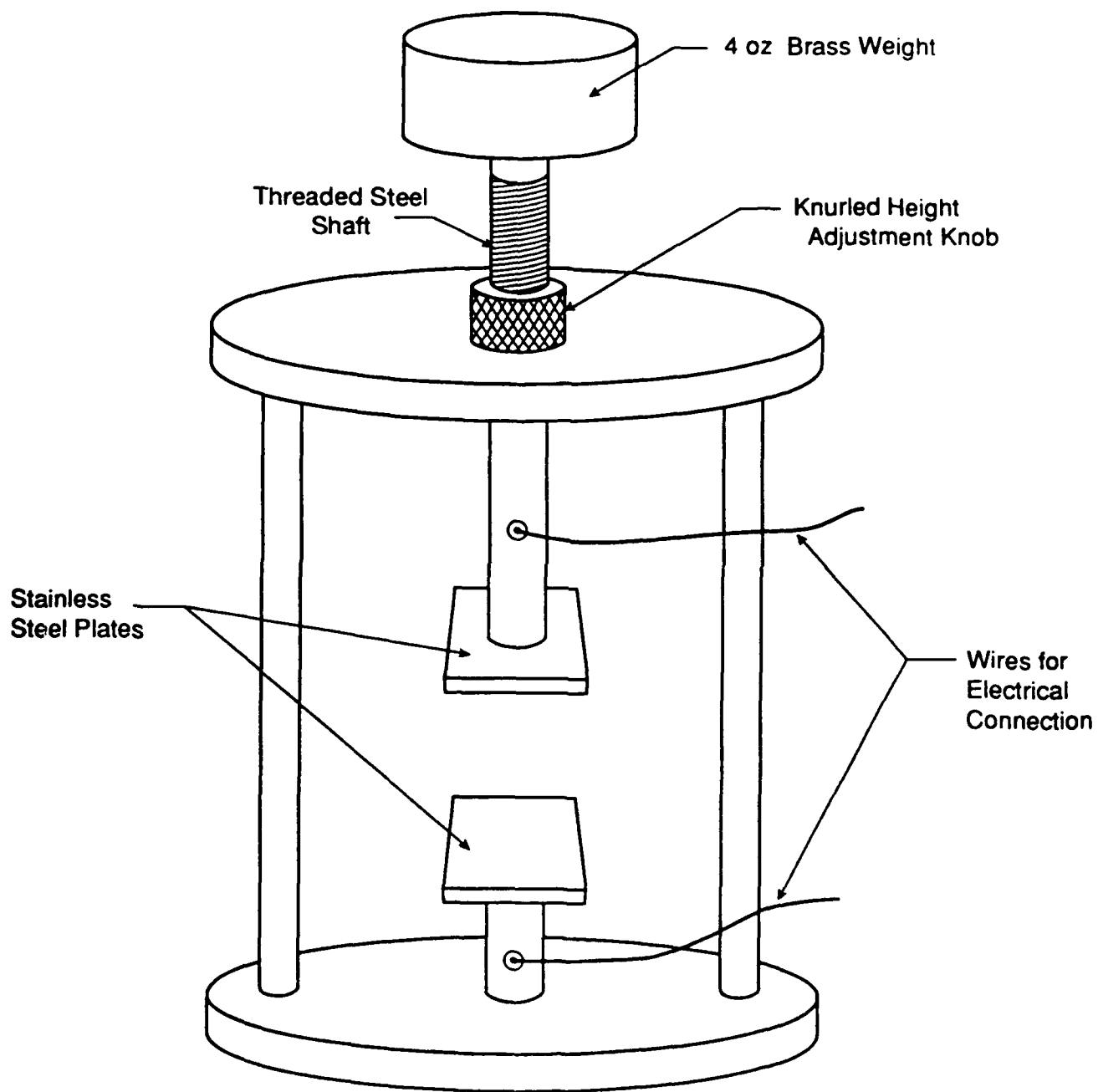


Figure 1. Setup for Conductivity Measurements by Impedance.

Impedance Spectroscopy. The AC impedance measurement of the Ni/Polymer/Ni cell was conducted using EG&G, Princeton Applied Research Model 368, AC Impedance Meter.

Conductivity Measurements. Conductivity measurements of the free-standing polymer electrolyte films were made using the apparatus shown in Figure 1. With the top plate of the conductivity apparatus (Figure 1) in the raised position, the polymer electrolyte film was laid out flat on the bottom, stainless steel electrode. A piece of nickel foil (cut to the same size as the stainless steel electrode, 5.264 cm²) was placed over the top of the polymer electrolyte film and smoothed to insure good contact with the electrolyte film. The top plate was lowered so that it was in contact with the Ni foil and the weight (approximately 1000 g) was placed on top of the apparatus. To prevent the weight from extruding the gel, the brass knob on the shaft of the top plate was lowered so that it was just in contact with the top of the conductivity apparatus. The conductivity apparatus was then placed into a glass vacuum cell and the appropriate electrical connections were made. The glass cell was sealed, using a mechanical clamp, while in the dry box and the impedance was measured from 5 Hz to 100 KHz using the impedance spectrometer outside the dry box.

After measuring the impedance the glass vacuum cell containing the conductivity cell was returned to the dry box. The polymer electrolyte film was removed and the gap between the two parallel plates of the conductivity cell was measured with a thickness gage. The thickness of the Ni foil (0.0014 cm) was subtracted from this measurement and the remainder was reported as the thickness of the tested polymer electrolyte film.

Conductivity of solutions was measured using a Rosemont Analytical Conductivity cell, Model No. CEL-G10; cell constant, K=10; approximate capacity 5 mL. YSI 3165 conductivity calibration solution, consisting of potassium chloride, 6.582 percent; and iodine, 0.0002 percent; dissolved in water, was used to determine the cell constant. The conductivity of this solution at 25°C is adjusted at 10⁻¹ S/cm ± 0.25 × 10⁻⁶ with a cell constant equal to 10. The cell constant at other than room temperature was calculated from the following equation:

$$\text{Cell Constant} = (\text{conductivity at } 25^{\circ}\text{C}) \times (A + Bt + Ct^2)$$

where t = temperature in °C

$$A = 0.5825$$

$$B = 0.0157$$

$$C = 0.00040$$

Conductivity of the calibration solution at different temperatures, as calculated by the above equation is shown in Figure 2.

Cyclic Voltammetry (CV). A solution consisting of ten percent by weight of LiBF_4 in NMP was made in the dry box. IR spectra indicated that the solution was relatively water free. The lithium surface was cleaned with hexane and used as the working electrode, the counter electrode, and the reference electrode. Additional experiments were performed substituting a platinum wire (cleaned with nitric acid) for the working electrode. CV was performed at two scan rates at 5 mV/sec and 20 mV/s in the range +3.0 volts to -3.0 volts.

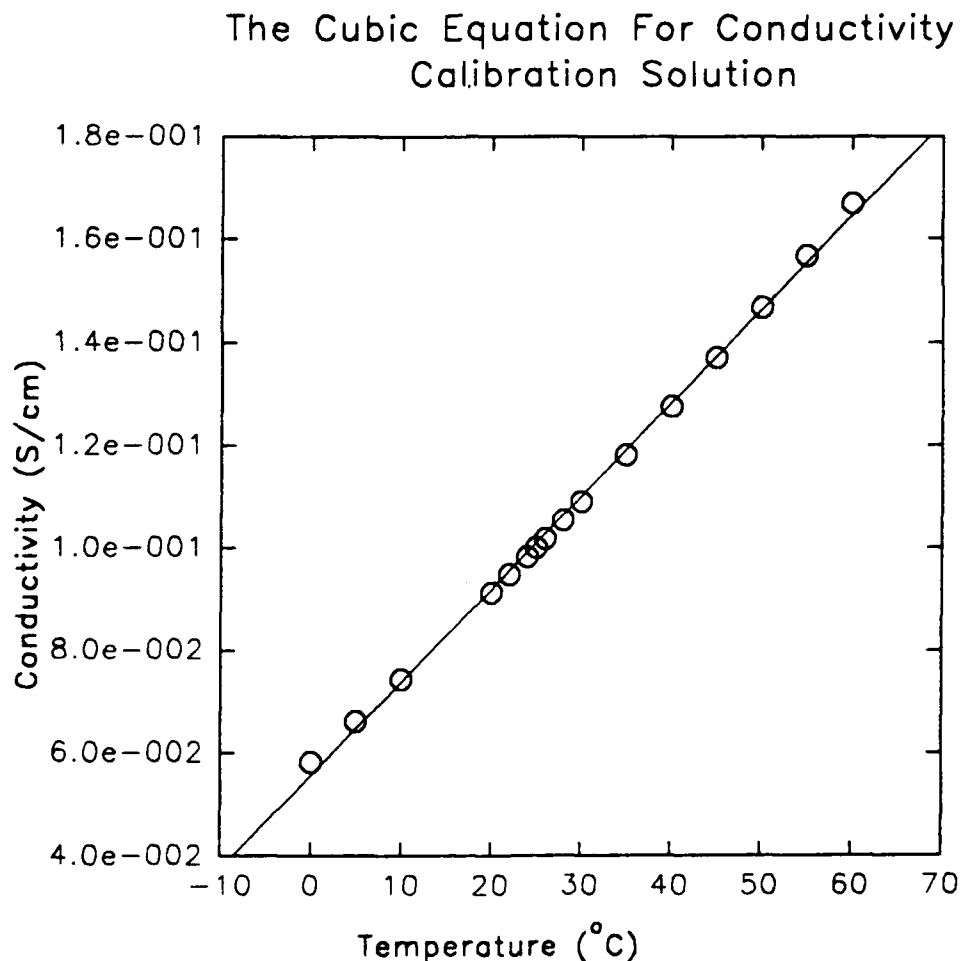


Figure 2. Conductivity of Aqueous Potassium Chloride Solution at Different Temperatures for Calibration of Cell Constant.

4. RESULTS AND DISCUSSION

The objective of the present research was to study the effect of the different parameters on the conductivity of the gel electrolytes. The parameters studied are (a) the ratio of lithium salt to the polymer, (b) ratio of polymer to the organic plasticizer, and (c) ratio of organic plasticizer to salt. The effect of temperature on conductivity of the lithium salt in the (a) plasticizer only, (b) with polymer in solution and (c) in the heterogeneous film as gel electrolytes were also carried out and the energy of activation (E_a) for (a), (b), and (c) were determined.

It was expected that measurement of the E_a at different stages of processing of the gel electrolyte, as mentioned above, would shed some light on the roles of the aforementioned parameters on ion transport.

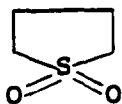
Selection of Host Polymer. Polyacrylonitrile, a homopolymer of acrylonitrile monomer has been widely used in gel electrolyte studies [5,18-21,28]. Although conductivities in the range of 10^{-3} to 10^{-4} S/cm at room temperature are reported, the preparation of hybrid electrolyte from this polymer is rather difficult due to insolubility of this polymer to common organic solvents that would also dissolve the inorganic lithium electrolytes. Also, high polarity of closely spaced nitrile groups cause a high glass transition temperature (T_g) in the vicinity of 100°C . In the present study a copolymer of acrylonitrile and butadiene (NBR) having lower T_g has been used as the host polymer. Spacing of the nitrile groups decreases dipolar interaction. Decreasing dipolar interaction increases the free volume which decreases T_g . Lower free volume would facilitate segmental motion of the polymer chain at lower temperatures, which should promote ion transport at the ambient temperature. It is well known in the rubber industry that T_g of NBR copolymers increases with the proportion of nitrile group in the copolymer. However, decreasing acrylonitrile also decreases the number of lithium coordination sites, so there may be an optimum between these opposing requirements of low T_g versus high concentration of nitrile groups.

Specific Conductivity of Inorganic Salts in Different Organic Plasticizers. Three inorganic salts were used in preliminary experiments. These are lithium tetrafluoroborate (LiBF_4), lithium trifluoromethane sulfonate (LiCF_3SO_3), and lithium hexafluoroarsenate (LiAsF_6). The plasticizers used are considered for this work and their chemical formulae are presented in Figure 3.

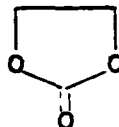
Sulfolene



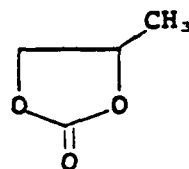
Sulfolane



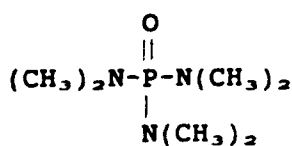
EC



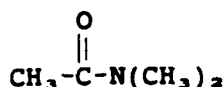
PC



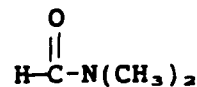
HMPA:
Hexamethyl
-phosphoramide



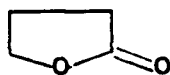
DMAC:
Dimethylacetamide



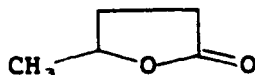
DMF:
Dimethylformamide



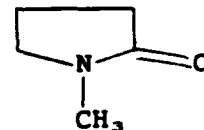
γ -Butyrolactone



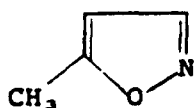
γ -Valerolactone



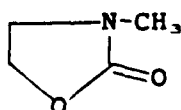
N-Methyl-pyrrolidinone



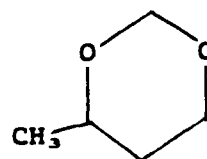
5-Methylisoxazole



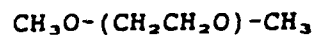
3-Methyl
-2-oxazolidinone



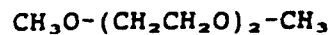
4-Methyl-1,3-dioxane



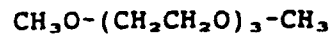
Dimethyl-monoglyme



Dimethyl-diglyme



Dimethyl-triglyme



Dimethyl-tetraglyme



Figure 3. Chemical Formulae of the Plasticizers Used.

The DC conductivity data at 25°C for 1 to 5 percent solutions of LiBF_4 , LiAsF_6 and LiCF_3SO_3 in different plasticizers are recorded in Tables 2, 3, and 4, respectively. The corresponding percent concentration (by weight) vs specific conductivity plots are shown in Figures 4, 5, and 6 for LiBF_4 , LiAsF_6 , and LiCF_3SO_3 , respectively.

In selecting a plasticizer, the following factors were also taken into consideration:

- | | |
|---|------------------------------|
| (1) Freezing point $\leq -40^\circ\text{C}$ | (4) Solvate lithium salts |
| (2) Boiling point $\geq 175^\circ\text{C}$ | (5) Low viscosity |
| (3) Not reactive to lithium | (6) High dielectric constant |

The melting and boiling temperature of the plasticizers used are presented in Table 5. It is apparent that both DMF and DMAC have too a low boiling point to satisfy the above criteria, although they have the highest conductivity (Table 2, 3, 4 and Figures 4, 5, and 6). Also, DMF has been reported to have some reactivity with lithium. γ -butyrolactone and 4-methyl-1,3-dioxane showed a pale yellow collar in the presence of lithium salts, indicating a side reaction. Sulfolene, sulfolane and HMPA as well as ethylene carbonate have too high a melting point. The 5-methyl isoxazole, 3-methyl-2-oxazolidinone and 4-methyl-1,3-dioxane are too expensive, although they have moderately high conductivity (Table 2). The last four plasticizers, glymes (methoxyethyl ethers), have the lowest conductivity. This is ascribed to the low dielectric constant of these plasticizers. Figure 7 shows conductivity vs molar ratio of LiBF_4 in 2-methoxyethyl ether. The maximum in conductivity occurs as the molar ratio of plasticizer: LiBF_4 approaches 4 (as compared to 8:1 for polyethylene oxide). The decrease in conductivity beyond the maximum may be ascribed to ion-pair formation.

Data for dielectric constant and viscosity of some common plasticizers are shown in Table 6^[28]. The ether-type plasticizers would have similar dielectric constant as in PEO_{400} (approximately five), which is the lowest among the plasticizers listed. This would promote ion-pair formation. The fact that the maximum occurs at $\text{PEO}:\text{Li}=8$ vs 2-methoxyethylether: $\text{Li}=4$, may be due partly to the widely different mobilities of the ions in the monomeric plasticizer and the polymer.

TABLE 2
SUMMARY OF CONDUCTIVITY DATA (1-5%LiBF₄)
IN DIFFERENT PLASTICIZERS

Solvent	Conductivity (ohm x cm ⁻¹ x 10 ⁴) at 25°C				
	5% LiBF ₄	4% LiBF ₄	3% LiBF ₄	2% LiBF ₄	1% LiBF ₄
mono-EGDME	12.7	8.95	7.01	4.0	0.80
di-EGDME	18.6	13.9	10.0	5.0	1.96
tri-EGDME	---	---	---	---	0.20
tetra-EGDME	6.86	5.96	3.9	3.0	0.80
γ-butyrolactone	67.6	62.6	55.2	42.1	28.2
N MP	63.7	55.7	49.1	32.1	21.2
HMPA	---	---	---	---	16.1
DMAC	133.0	115.0	99.2	74.1	44.4
γ-valerolactone	40.2	37.8	37.1	30.2	19.2
DMF	169.0	145.0	122.0	89.7	50.0
PC	36.3	38.8	33.9	31.2	22.5
5M-isoxazole	61.7				
3M-2-oxazolidinone	66.4				
4M-1,3-dioxane	66.0				

At 5% LiBF₄

Trend:DMF > DMAC >> BL 3M-2-oxazolidinone 4M-1,3-dioxane, NMP 5M-isoxazole >>
PC >> Di-EGDME > Mono-EGDME >> Tetra-EGDME

At 1% LiBF₄

Trend:DMF > DMAC >> BL > PC~NMP > VL > HMPA >> Di-EGDME > Mono-EGDME
tetra-EGDME > Tri-EGDME

TABLE 3
SUMMARY OF CONDUCTIVITY DATA (1-5% LiAsF₆)
IN DIFFERENT PLASTICIZERS

Solvent	Conductivity (ohm x cm ⁻¹ x 10 ⁴) at 25°C				
	5%	4%	3%	2%	1%
di-EGDME	---	6.06	5.06	3.0	0.995
γ-butyro-lactone	63.3	53.5	43.3	29.1	15.0
N MP	39.8	33.3	26.3	18.1	9.95
DMAC	79.6	66.7	51.6	33.1	17.9
γ-valero-lactone	48.0	40.4	32.4	23.1	11.9
DMF	104.0	81.8	63.8	43.1	22.9
PC	43.9	37.4		22.1	10.9

Trend: DMF > DMAC > BL > VL > PC NMP >> Di-EGDME

TABLE 4
SUMMARY OF CONDUCTIVITY DATA (1-5% LiCF₃SO₃)
IN DIFFERENT PLASTICIZERS

Solvent	Conductivity (ohm x cm ⁻¹ x 10 ⁴) at 25°C				
	5%	4%	3%	2%	1%
di-EGDME	8.16	6.06	4.05	3.04	0.995
γ-butyro-lactone	37.8	34.3	29.5	24.1	15.0
N MP	41.9	36.4	28.3	19.1	10.9
DMAC	91.0	75.8	60.7	43.1	22.9
γ-valero-lactone	24.5	22.2	20.2	16.0	9.95
DMF	108.0	88.9	68.8	48.1	26.9
PC	21.4	20.2	17.7	15.0	9.95

Trend: DMF > DMAC > BL > NMP > VL ~ PC >> Di-EGDME

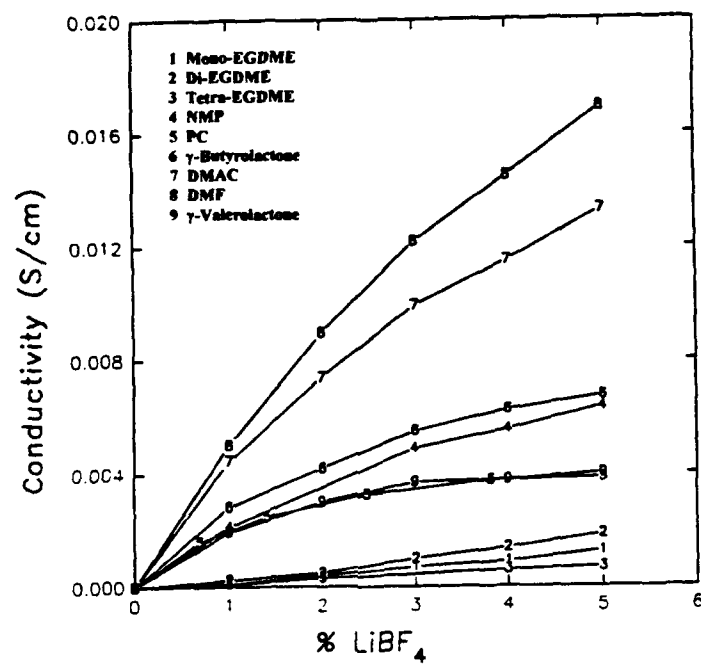


Figure 4. Conductivity of LiBF_4 in Different Plasticizers.

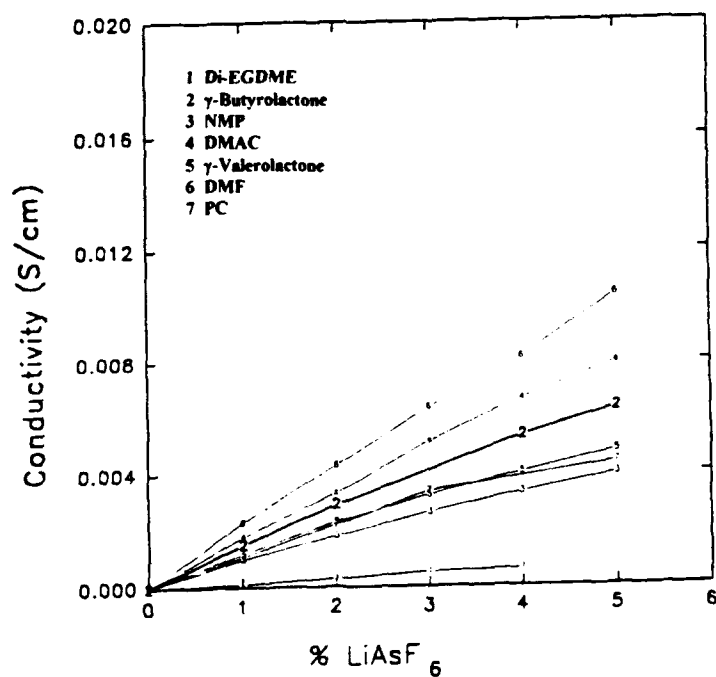


Figure 5. Conductivity of LiAsF_6 in Different Plasticizers.

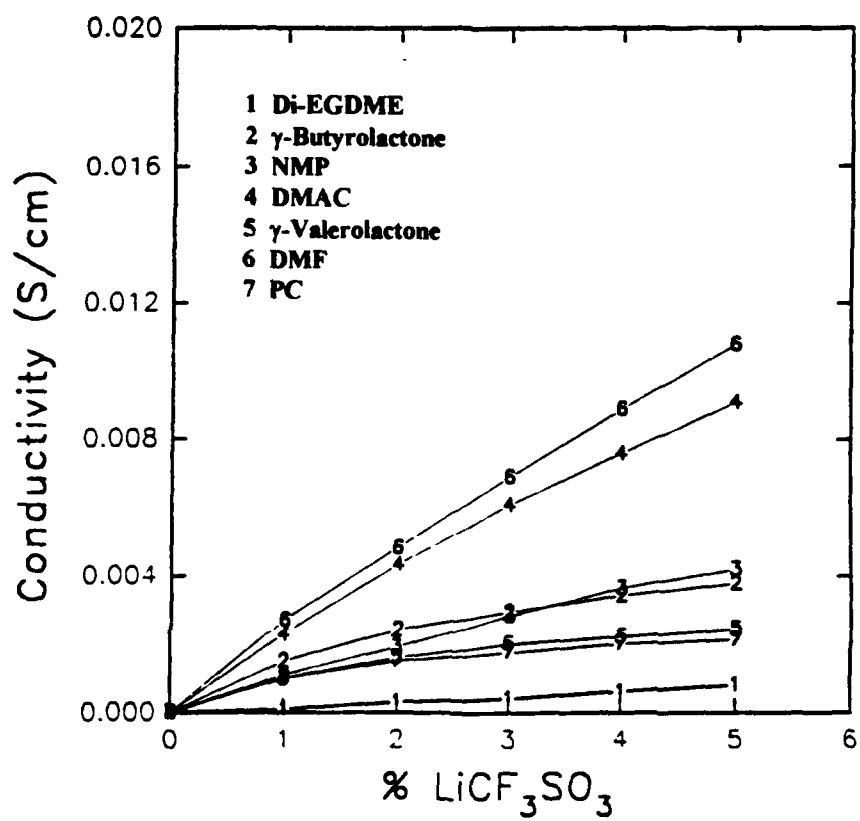


Figure 6. Conductivity of LiCF₃SO₃ in Different Plasticizers.

TABLE 5
MELTING AND BOILING POINTS OF DIFFERENT PLASTICIZERS

	bp (°C)	mp (°C)
Sulfolene (98%)	--	65
Sulfolane (99%)	285	27
HMPA (99%)	231 / 740mm	7
γ -Butyrolactone (99+%)	204	-45
γ -Valerolactone (99%)	207	-31
DMF	153	-61
DMAC	165	-20
NMP	81 / 10mm	-24
EC	243 / 740mm	38
PC	240	-55
5-Methylisoxazole	122	--
3-Methyl-2-oxazolidinone	87 / 1mm	15
4-Methyl-1,3-dioxane	114	-45
dimethyl-monoglyme	85	-58
dimethyl-diglyme	162	-64
dimethyl-triglyme	216	-45
dimethyl-tetraglyme	275	-30

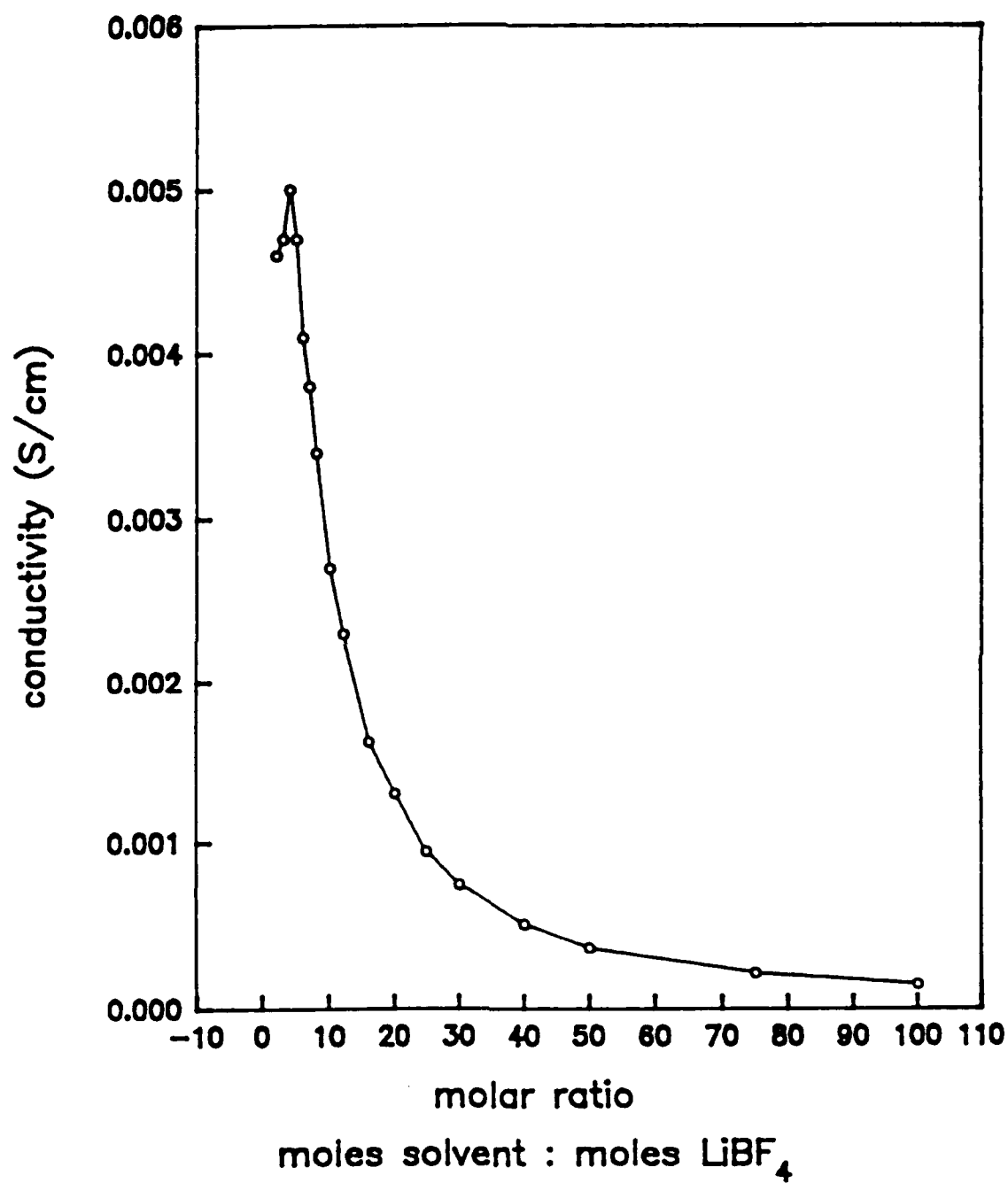


Figure 7. Conductivity of LiBF₄ in 2-Methoxyethyl ether

TABLE 6
PHYSICAL DATA FOR SOME PLASTICIZERS AND HOST MATERIALS^{a,b}

Solvent	Dielectric constant, ϵ at 25°C	Viscosity (cP)
DMF	36.7	0.80
PC	64.4	2.53
EC	89 ^a	1.90
γ BL	39.1	1.75
H ₂ O	78.5	1.00
PEO ₄₀₀	5	3
PAN	6.5 ^c	--
NMP ^c	32.2	1.65

^a From Gray [28]

^b Measured at 40°C

^c From manufacturer data (GAF) measured at 25°C

It is interesting that NMP has both lower dielectric constant and viscosity than γ -butyrolactone, but equal or lower conductivity (Figures 4-6). This indicates the existence of other criteria for ionic conductivity (e.g., interaction with Li⁺). The dielectric constant and viscosity of DMF is about half and one-third of those of PC. Lower dielectric constant should favor more ion-pair formation (lower conductivity) whereas lower viscosity should give higher ion mobility (higher conductivity). The fact that conductivity of DMF is much higher than PC (Figures 4-6) may indicate the predominant effect of viscosity.

The plasticizers for further evaluation are γ -valerolactone, NMP and PC. Figures 4, 5, and 6 show they have comparable conductivity, with NMP having slightly higher conductivity except for LiAsF₆. Both γ -valerolactone and PC have been used with limited success as a plasticizer for gel electrolyte in earlier work. Therefore, NMP was chosen as the plasticizer for this study.

Recently, some work has been carried out using a blend of PC/EC as plasticizer for gel electrolyte^[29]. Table 7 shows conductivity data with 50:50 blend of PC with another plasticizer from the list in Table 6. Interestingly, NMP shows the highest conductivity after DMF and DMAC, which were not suitable because of their low boiling point. The

TABLE 7
SUMMARY OF CONDUCTIVITY DATA OF TWO-PLASTICIZER
SYSTEM (50:50) WITH 3% LiBF₄

No.	Solvent 1	Solvent 2	Conductivity (ohm x cm ⁻¹ x10 ⁴)
21	PC	EC	42.6
22	PC	Sulfolene	21.3
23	PC	Sulfolane	22.3
24	PC	γ -Butyrolactone	47.5
25	PC	NMP	62.0
26	PC	DMAC	81.7
27	PC	γ -Valerolactone	37.4
28	PC	DMF	92.5
29	PC	5-methyl-isoxazole	51.2
30	PC	4-methyl-1,3-dioxane	28.5
31	PC	3-methyl-2-oxazolidinone	50.2

conductivity of the PC/NMP blend is also higher than either PC or NMP at the same concentration (3%) of LiBF_4 (cf. Tables 2 and 7), which is an additional reason to choose NMP as the plasticizer for this work

Conductivity of the three lithium salts, LiBF_4 , LiAsF_6 and LiCF_3SO_3 in NMP is presented in Figure 8. It may be observed that conductivities of LiAsF_6 and LiCF_3SO_3 are comparable to each other whereas that of LiBF_4 is slightly higher. Molecular weight for the three salts is 93.75, 195.85, and 156.01 for LiBF_4 , LiAsF_6 , and LiCF_3SO_3 , respectively. The higher conductivity of LiBF_4 may be due to the availability of a larger number of lithium ion at the same percent concentration, the difference in dissociation of the salts, or both. The difference in dissociation is indicated for LiAsF_6 and LiCF_3SO_3 which differ significantly in molecular weight but show approximately the same conductivity.

Figure 9 shows the conductivity of LiBF_4 in different plasticizers up to a concentration of 16% LiBF_4 by weight. As expected, conductivity shows a maxima with concentration, which is at a different concentration for different plasticizers. Except for DMF and DMAC, NMP shows higher conductivity than the other plasticizers studied.

Selection of the NBR Copolymer. Preliminary screening of the conductivity data for the selection of a polymer was carried out using DEA. The polymer film was made on the single surface electrode itself by covering the electrode with a few drops a 3% solution in DMF or NMP, drying inside a vacuum oven (500 mm Hg at room temperature), followed by high vacuum (75 mm Hg) at 80°C. Table 8 shows the solubility of NBR copolymers in different solvents.

Conductivities were measured between -100 to 100°C. A summary of electrical conductivity data of NBR copolymers in the +75 to -75°C range are presented in Table 9. The changes of conductivity with temperature have a maximum around $\pm 25^\circ\text{C}$ range. The maximum could not be correlated with any morphological change in the polymer (e.g., T_g). This is discussed in Appendix B. Data submitted in Table 9 do not indicate a definite trend. Conductivity is also influenced by the solubility of the sample, as in 1000X132 (Table 9) which has the highest ACN content (50.5%) but is sparingly soluble in DMF (Table 8). It has lower conductivity than 1000X88 which has lower ACN content (44%). If Nipol 1000X132 is excluded from Table 9, Nipol 1000X88 and Zetpol 1020, which have the highest ACN, would also have the highest overall conductivity. However, the trend is not clear and the conductivity difference is small. Zetpol 1020, having less unsaturation would be more resistant to weather. Also, its solubility in NMP (the plasticizer chosen) is adequate

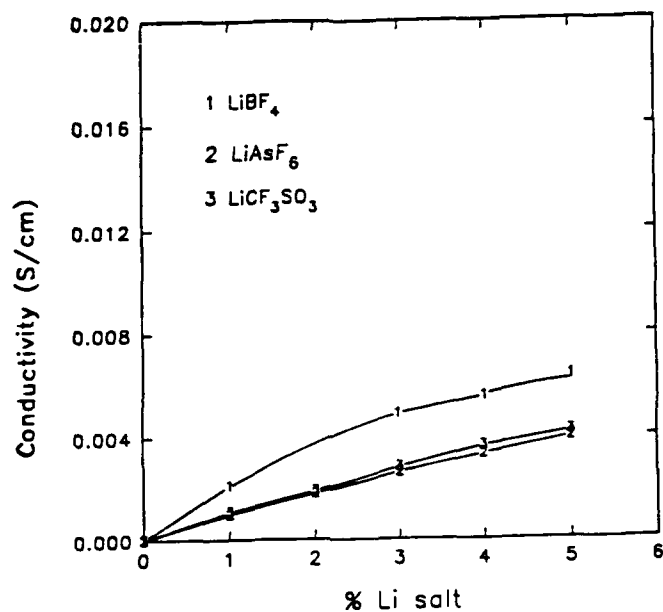


Figure 8. Conductivity of Different Lithium Salts in NMP.

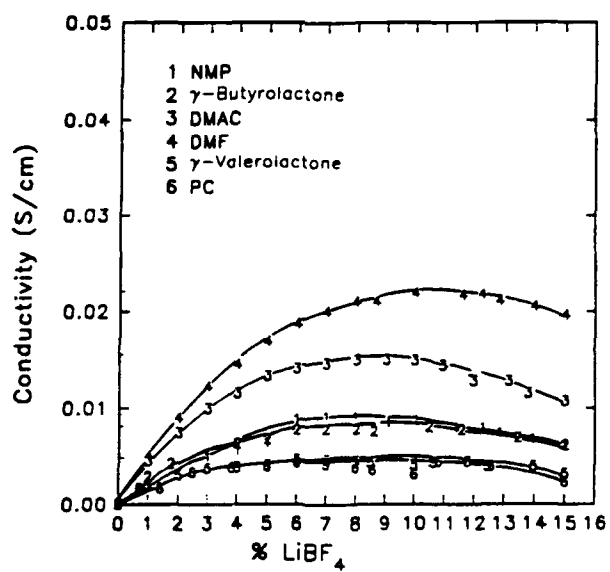


Figure 9. Conductivity of LiBF_4 vs Concentration in Different Plasticizers.

TABLE 8
SOLUBILITY OF NBR COPOLYMER IN DIFFERENT SOLVENTS

	DMF	DMAC	MEK	Acetonitrile
Nipol-1000X88*	3% sol		3% sol	1% insol
Nipol-1000X132*	3% cloudy* 2% cloudy	2% cloudy	3% insol	1% insol
Nipol-1034-60*	1% insol		3% cloudy	1% insol
Nipol-1453HM*	2% cloudy	2% cloudy	2% cloudy	
Nipol-1401LG	3% sol		3% cloudy	1% insol
Nipol-1432	3% sol		3% sol	1% insol
PAN	3% sol		1% insol	1% insol
Polyox N750			1% insol	1% sol
Zetpol-1020*	3% sol			

* milled sample

TABLE 9
CONDUCTIVITY OF NBR AND HNBR ELASTOMERS WITH LiBF_4
(CN:Li=8) AT VARIOUS TEMPERATURES AT 10^5 Hz

		Conductivity (mhos/cm $\times 10^9$)				
Sample ID, C:Li 8:1	ACN (%)	-75°C	-25°C	0°C	25°C	75°C
PAN		1.3	20.0	200.0	31.6	31.6
Nipol-1000X132	50.5	3.2	15.8	79.4	25.1	31.6
Nipol-1000X88	43.9	1.0	100.0	316.0	50.1	79.4
Nipol-1401 LG	40.9	1.0	2.5	20.0	15.8	12.6
Nipol-1432	33.2	1.3	6.3	15.8	12.6	6.3
Nipol-1034-60	21.3	3.2	7.9	50.1	7.9	20.0
Zetpol-1020	44.5	2.0	31.6	631.0	63.1	39.8

for making a film. Zetpol 1020 (hereon referred to as HNBR) was therefore selected for further work in the study.

Specific Conductivity of Gel Electrolyte by DC Conductivity. The role of the polymer in the gel electrolyte system consisting of polymer/plasticizer/inorganic salt is still not completely resolved. It is generally anticipated that the polymer only acts as a stiffener for the low molecular weight, high dielectric constant, and low viscosity plasticizer, which solvate the salt and is the conducting medium. Watanabe et al.^[21] and Reich and Michaeli^[29] observed that the energy of activation for ion transport is largely independent of polymer concentration. This suggests an ion migration largely through the plasticizer domain which surrounds the polymer matrix. Residual conductivity in the polymer has been anticipated to be the result of ion-hopping between localized sites, although the salt is largely dispersed as ion-pairs through the polymer^[30]. However, non-Arrhenius behavior is observed in some systems, e.g., Viton/PC/LiClO₄^[31], which indicates participation of the polymer.

In the present study the E_a for ion transport was determined for the salt in the plasticizer without the polymer. The effect of polymer was then examined (1) with the polymer dissolved in the plasticizer along with the salt and (2) as a film containing the swollen plasticizer and the salt. Table 1 shows the composition of the electrolytes used for homogeneous solutions.

Figure 10 illustrates the conductivity of the electrolyte consisting of HNBR44/LiBF₄/NMP as a function of molar ratio of HNBR/Li at temperatures ranging from 0 to 60°C. NMP concentration is 15 times that of the polymer to form a homogeneous solution (Table 1). It may be observed that conductivity decreases with higher ratio of the polymer. This may be ascribed mainly to lower lithium concentration at higher polymer lithium ratio.

An increase in conductivity with salt (LiBF₄) concentration was shown in Figure 4. Figure 11 shows the effect of temperature (Arrhenius plots) for three concentrations of LiBF₄ in NMP, including a 15% concentration not tested before. In agreement with Figure 4, conductivity increases from 2.5 to 8% LiBF₄. At 15% LiBF₄, a decrease of low temperature conductivity is observed, presumably due to ion association at high concentration. Ionic dissociation increases with temperature. Consequently, the slope of the Arrhenius plot is different from that at 2.5 and 8%. The E_a values calculated are 0.11, 0.13, and 0.19 eV/mole for 2.5, 8, and 15% LiBF₄, respectively. This shows that maximum

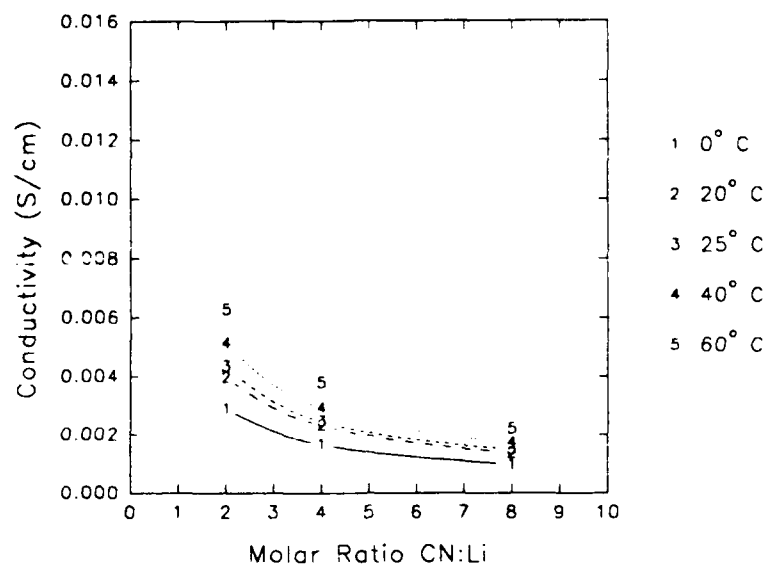


Figure 10. Conductivity vs Molar Ratio of HNBR/LiBF₄ in NMP at Various Temperatures.

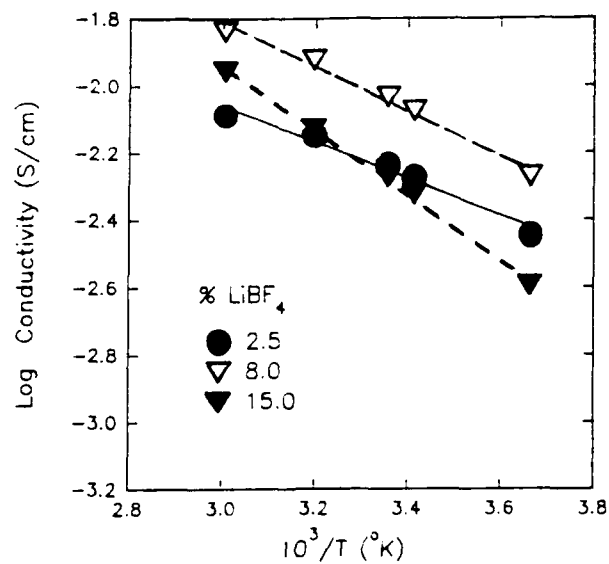


Figure 11. Arrhenius Plot of Log Conductivity vs $1/T$ (K) of Different Concentrations of LiBF₄ in NMP.

conductivity at room temperature should be observed somewhere between 8 and 15 percent LiBF_4 . The increase of the E_a at 15 percent LiBF_4 may be ascribed to the extra energy needed for ion dissociation.

Figure 12 shows the Arrhenius plot of log conductivity vs $1/T$ for solutions of HNBR (6.25 percent) in DMAC, BL, and NMP. The polymer:lithium salt ratio was maintained at 8:1 in all three solutions. Although conductivity values are higher in DMAC than in the other plasticizers (as would be expected), the parallel lines show that the E_a values are about the same. If it is presumed that at the dilute ionic concentration (0.6% LiBF_4) the salt is fully dissociated in all the plasticizers shown, the conductivity increase may be ascribed to an increase in mobility due to either higher temperature or lower viscosity of the solutions. Thus, the lower viscosity of HNBR solution in DMAC explains its higher conductivity. The E_a values calculated from the slopes are 0.10 eV/mol for DMAC and NMP and 0.09 eV/mol for BL. These values are comparable to 0.11 eV/mol for 2.5% LiBF_4 solution in NMP.

Figure 13 shows the same plot with 2.5 percent LiBF_4 in NMP with and without 2:1 (CN:Li) HNBR. Although conductivity is much higher in NMP only, the activation energy is about the same (0.11 vs 0.10 eV/mol). This indicates absence of any influence of the polymer on E_a . The conductivity decrease in the presence of polymer may principally be ascribed to decreased mobility due to higher viscosity. It may be noted that conductivity of LiBF_4 in NMP in Figure 13 is slightly higher than that in Table 2. This is due to measurements at different times by different persons and may reflect variability in the chemicals and procedures.

Figure 14 shows the Arrhenius plots of the solutions in NMP where CN:Li ratio was varied. The amount of NMP was varied in proportion to the amount of polymer, in effect varying the concentration of LiBF_4 in NMP at a constant polymer concentration (Table 1). As expected, conductivity increases with temperature and as the lithium salt concentration in NMP increases. However, E_a remains more or less constant at 0.106, 0.112, and 0.112 eV/mol for 2:1, 4:1, and 8:1 CN:Li, respectively, with an average of 0.11 eV/mol. This again indicates that the presence of polymer does not influence the activation energy. The difference in conductivity in the three samples (Figure 14) is due to the difference in salt concentration arising from its dilution with larger amounts of NMP as the HNBR:Li ratio increases.

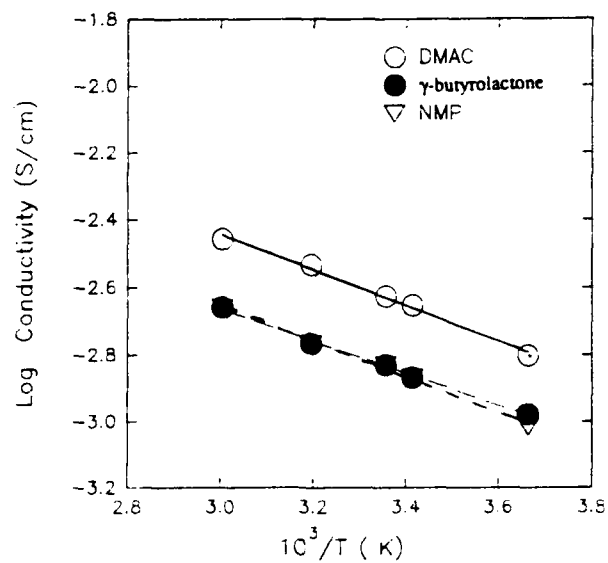


Figure 12. Arrhenius Plot of Log Conductivity vs 1/T (K) of HNBR/LiBF₄ (CN/Li=8) in Different Solvents.

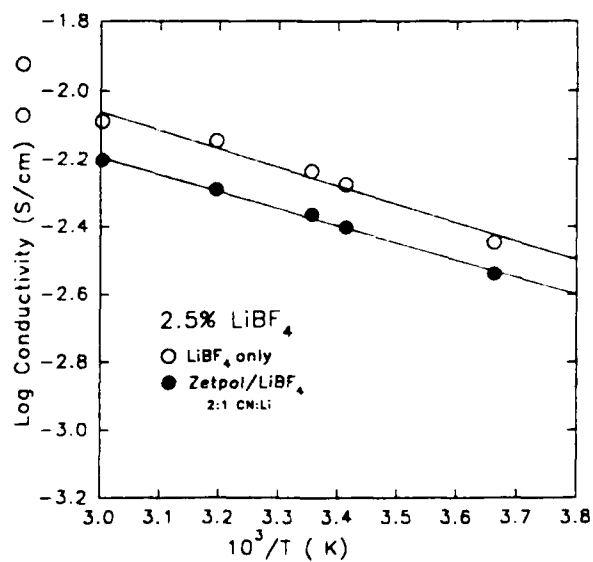


Figure 13. Arrhenius Plot of Log Conductivity vs 1/T (K) for LiBF₄ in NMP With and Without HNBR.

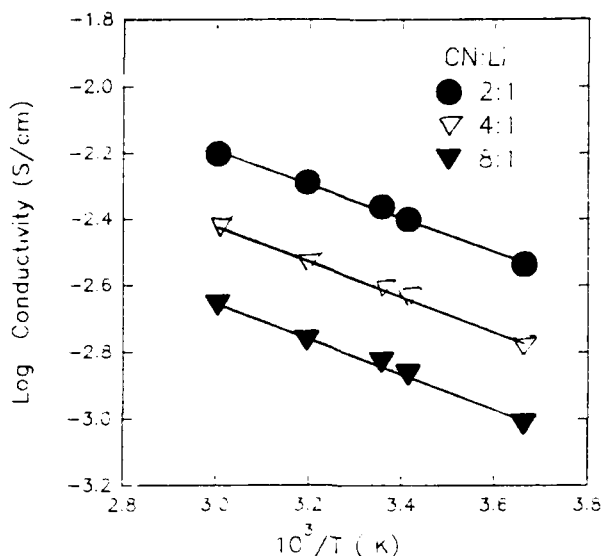


Figure 14. Arrhenius Plot of Log Conductivity vs $1/T$ (K) for Different Ratios of Polymer/Lithium in NMP.

It is significant that E_a does not change in different solvents (Figure 12), at different concentration of the salt in NMP (up to a limit, Figure 11), and in the presence of the polymer (Figures 13 and 14). The observation that the energy required for activation of ion transport does not change in the presence of the polymer indicates a mechanism involving the solvent with little interference by the polymer as long as the polymer is in solution. This does not, however, rule out interaction with the polymer, as increased viscosity was observed as the concentration of salt was increased at constant polymer:NMP concentration. However, as observed in Figure 14, this does not have any effect on E_a .

Conductivity of Hybrid Films by Impedance Measurement. Preparation of the hybrid films is described in the experimental section. The composition of different films made are shown in Table 10. The approximate composition was arrived at by measuring the initial and final weight after pressing the film and assuming that liquid leached out is the solvent with the initial concentration of the lithium salt.

TABLE 10

COMPOSITION VS IONIC CONDUCTIVITY OF HYBRID FILMS

Sample CN:Li Mole	NMP: HNBR wt.	CN:Li: NMP	Weight Before Pressing	Weight After Pressing	Weight Lost	Temp (°C)	Thickness (cm)	Area (cm ²)	Resistivity (Ω-cm)	Conductivity (S/cm x 10 ⁻⁴)	Comments
2:1*	3:1		0.727	0.366	0.361	19	0.0164	5.264	---	---	
2:1*	3:1	2:1:6.58	0.699	0.368	0.331	21	0.0494	5.264	5311	1.88	NMP Separated
2:1*	3:1		0.7	0.389	0.311	21	0.0519	5.264	4209	2.38	
2:1*	3:1		0.725	0.329	0.396	21	0.0342	5.264	6964	1.43	
3:1	3:1		0.773	---	---	---	---	---	---	---	Too soft, no sep.
4:1	2.25:1		0.683	---	---	---	---	---	---	---	Too soft, no sep.
4:1*	2:1		0.706	0.51	0.196	21	0.0443	5.264	2575	3.88	
4:1*	2:1	4:1:8.73	0.733	0.552	0.181	21	0.0469	5.264	2697	3.71	No Separation
4:1*	2:1		0.716	0.507	0.209	21	0.0367	5.264	3390	2.95	
4:1*	1.5:1		0.701	0.592	0.109	20	0.0443	5.264	6741	1.48	
4:1*	1.5:1	4:1:6.55	0.675	0.558	0.117	20	0.0443	5.264	7591	1.32	No Separation
4:1*	1.5:1		0.652	0.535	0.117	20	0.0443	5.264	7782	1.29	
4:1*	1.75:1		0.844	0.745	0.099	20	0.04204	5.264	5203	1.92	
4:1*	1.75:1	4:1:7.64	0.876	0.769	0.107	20	0.04458	5.264	2779	3.6	1 min Press Time
4:1*	1.75:1		0.868	0.763	0.105	20	0.04458	5.264	5667	1.765	
3:1*	1.75:1		0.823	0.7	0.123	20	0.03924	5.264	10246	0.976	
3:1*	1.75:1	3:1:5.73	0.57	0.412	0.158	20	0.024	5.264	10709	0.934	No Separation
3:1*	1.75:1		0.545	0.427	0.118	20	0.04432	5.264	12603	0.793	
3:1*	1.75:1		0.575	0.441	0.134	20	0.03924	5.264	19877	0.503	
8:1\$	1.5:1		---	---	---	20	0.0381	5.264	4746	2.11	
8:1\$	1.5:1	8:1:13.1	---	---	---	20	0.0381	5.264	3986	2.51	No Separation
8:1\$	1.5:1		---	---	---	20	0.00381	5.264	2849	3.51	

* Film pressed between non-porous teflon

Film pressed between porous teflon

\$ Formula too sticky to produce a free-standing film

The conductivity was determined from complex impedance measurements. The bulk resistance between stainless steel electrodes obtained from the real component of the plot is shown in Figure 15. The bulk resistance of the electrolyte along with thickness of the sample and electrode area yields the resistivity and its inverse, the conductivity. It may be observed that the bulk resistance shows as a spike in the real component of resistance. This is rather common for gel electrolytes and was observed by many other studies. It may be observed in Figure 15 that conductivity decreases (resistivity increases) with time. Figure 16 shows the plot of conductivity vs time. The decreased conductivity vs time was observed by other earlier workers^[32,33] and was attributed to loss of solvent by evaporation or changes in the nature and structure of the passivating layer. Conductivity decrease is parabolic. However, it does not yield a straight line with $t^{1/2}$, as the study of Tranchant et al.^[34]

Since the conductivity changes with time, it is difficult to compare samples of different compositions. However, conductivity after a constant interval is reproducible among the different specimens of the same composition. For example, conductivities of the three samples with 4:1 CN:Li and 1.5:1, NMP:HNBR after 10 minutes are 1.48, 1.32 and 1.29 S/cm (Table 10). Conductivities of different films were therefore compared after 10 minutes under compression in the sample holder.

According to Gray^[28], the electrolyte properties depend critically on the ratio of three components. It is not however possible to independently vary the components and still make a usable film. Polymer viscosity increases markedly with the concentration of LiBF_4 . At very high lithium concentration (CN:Li=1) it is difficult to dissolve the polymer in order to make a homogeneous film, whereas at low concentration of CN:Li the film gets too soft when a critical plasticizer concentration, dependent on CN:Li ratio, is exceeded. There is therefore a concentration window of NMP for each concentration of HNBR: LiBF_4 . It is conceivable that light cross-linking of HNBR would allow more plasticizer pickup without becoming too soft.

Table 10 and Figure 17 illustrate that at the CN:Li ratio of 4:1 conductivity increases as the plasticizer to salt ratio (Col. 3) increases. Although this conclusion is based on limited data, it agrees with the observation of Watanabe et al.^[21], with PAN as the host polymer. These investigators observed that the conductivity of the hybrid film increases with $[\text{EC}]/[\text{LiClO}_4]$ ratio, irrespective of PAN concentration. They attributed this to the increased ion mobility through the microphases of $[\text{EC}]/[\text{LiClO}_4]$. PAN is conceived to act only as a toughener until a limiting value of $[\text{EC}]/[\text{LiClO}_4] \approx 1.5$ is reached. At concentrations where

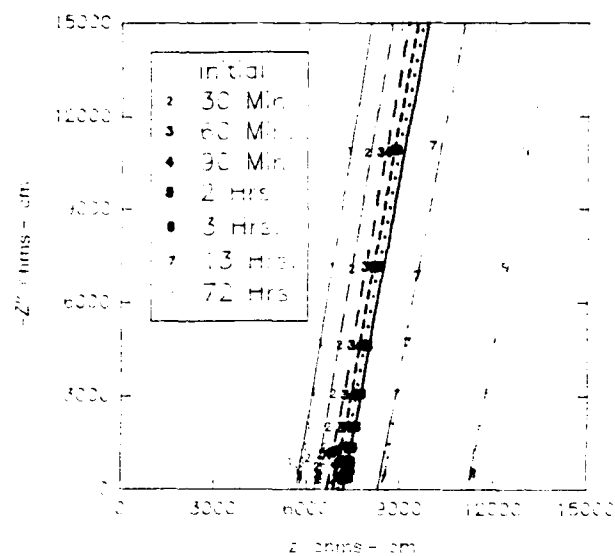


Figure 15. Conductivity of Hybrid Films by Complex Impedance Measurement.

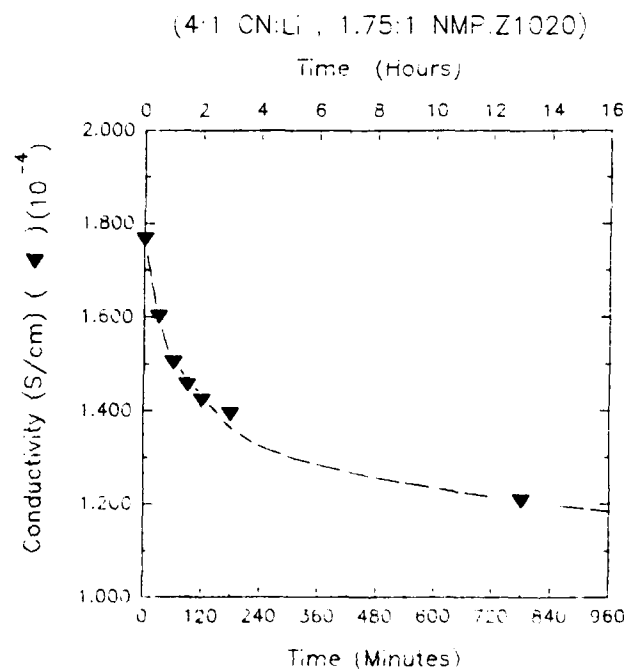


Figure 16. Conductivity of Hybrid Films vs Time by Impedance Measurement.

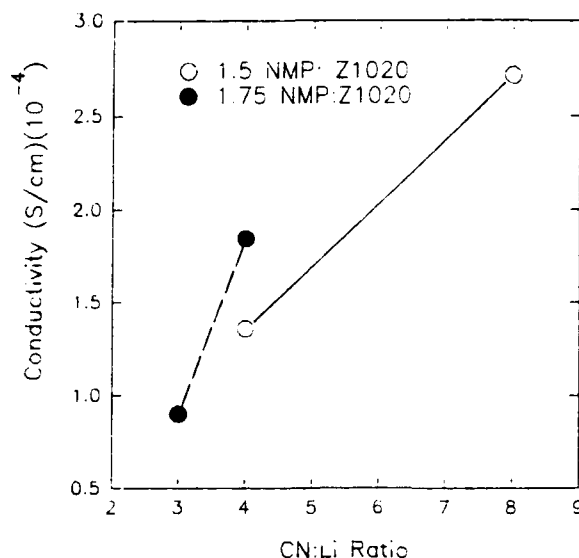


Figure 17. Conductivity as a Function of CN/Li Ratio and Plasticizer Concentration.

this ratio is lower than 1.5, PAN/LiClO₄ interaction is no longer negligible and conductivity decreases. The above observations are in broad agreement with our data. However, as observed in Figure 17 and Table 10, our data shows that conductivity increases with [plasticizer]/[salt] ratio only when the polymer:salt ratio is kept constant.

Conductivity of the polymeric electrolyte should increase as the number of charge carriers as well as the mobility of the ions increase. It is conceivable that mobility of the ions increases as the [plasticizer]/[salt] ratio increases (decreased viscosity) and decreases as the polymer:salt ratio decreases. Also, the salt is soluble both in the polymer and the plasticizer. It would be expected that conductivity will depend on the relative solubility and dissociation of ions in these phases (potential charge carriers) and the corresponding changes in the viscosity and mobility of the ions. The reason for the difference in our data to those of Watanabe, et al.^[21] may be attributed to the difference in the extent of interaction of HNBR and PAN with the lithium salt. However, more data are necessary to investigate the above trends and the optimum concentrations of the components for maximum conductivity. On comparing Figures 10 and 14 with 17, it may be observed that while conductivity decreases as the HNBR:LiBF₄ ratio increases when the polymer is in solution, an exactly opposite trend is observed when the components are in the form of a film. In this case, conductivity increases as the polymer to lithium ratio increases. However, a tremendous increase of

viscosity was observed as the polymer:lithium ratio decreases at constant weight percent polymer/NMP concentration. Greater complexation of both HNBR and NMP with lithium may be inferred, causing the viscosity to increase. An interaction of NMP and lithium was inferred from IR studies. Thus, the decreased conductivity with the decrease of polymer/lithium ratio may be attributed to the decreased mobility of ions caused by the tremendous increase of viscosity. Unfortunately, the optimum lithium concentration for maximum conductivity in films was not worked out. The highest room temperature conductivity observed is around 3.5×10^{-4} S/cm for 4:1:8.7 ratios in Table 10, as compared to 2.5×10^{-3} for a homogeneous solution at same CN:Li ratio and 5.8×10^{-3} for 2.5 percent LiBF_4 in NMP (Figures 11 and 12).

An Arrhenius plot of E_a for the 8:1:13 mole ratio of HNBR: LiBF_4 :NMP is shown in Figure 18. E_a is found to be 0.31 eV/mol, three times higher than the E_a observed for LiBF_4 in NMP (0.10 eV/mol, Figure 11) or in the homogeneous solution of NMP:HNBR (0.10 eV/mol, Figure 11 and 13). The fact that E_a remains constant for LiBF_4 solution in various solvents and in NMP, with and without HNBR, indicates that E_a increase in the film cannot be attributed solely to increased viscosity, and must be ascribed to the heterogeneous nature of the system. Thus, a mechanism involving both the polymer and the plasticizer may be inferred.

It appears that any mechanism for ionic conduction in the hybrid films has to include the extra energy needed to overcome the interphase resistance through the plasticizer/polymer phase boundary, the polymer/electrode interfacial resistance, and migration of ions through the plasticized solid. This may explain the higher E_a values for the hybrid film versus the solution in this study. It is conceivable that these resistances will change with composition. Thus, more E_a data at other HNBR:salt:plasticizers are necessary to obtain a clearer picture.

Watanabe, et al.^[21] observed decreased E_a , as the mole ratio of $[\text{E}_c]/[\text{LiClO}_4]$ was increased, irrespective of PAN concentration, until this ratio was lower than 1.5. As the ratio decreased further, E_a increased, indicating increased participation of the host polymer (more of the ionic species has to travel through the polymer phase). The total activation energy for ionic conduction should include ion-ion interaction energy, ion-polymer interaction energy, and the energy of formation of free volume for ion migration^[35]. The higher E_a values at low plasticizer/salt ratio was attributed to the high energy needed for the conducting species to interact with the immobilized polymer chains. In the case of HNBR, such participation seems to be occurring at a much higher plasticizer:salt ratio or lower polymer concentration. It may be noted that measurement temperatures in the case of PAN is lower than its T_g .

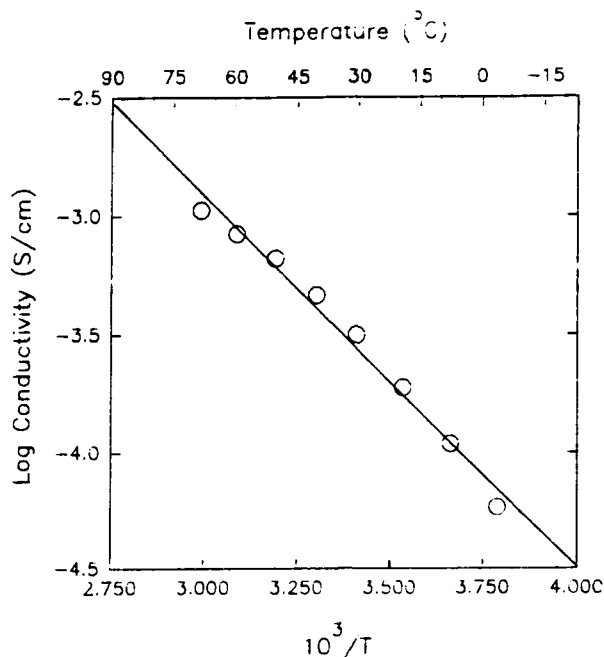


Figure 18. Arrhenius Plot of Log Conductivity vs $1/T$ (K) for the Hybrid Film, CN/Li/NMP=8/1/13.

while it is much higher than T_g in the case of HNBR. It is possible that the participation of HNBR in the conduction process at a lower concentration may be due to high flexibility of the chains, which allows easier interaction with the conducting species. The difference in interaction of PAN, NBR, and HNBR with LiBF_4 in the presence of NMP as revealed by IR measurements is discussed later. Interaction of LiBF_4 with NMP was also indicated in these studies, which introduces another factor to consider.

It may be concluded from this study that the polymer in the hybrid film does interfere in the ionic conduction process. However, the degree of its interference should depend on the specific polymer-electrolyte system and the concentration of the components.

Thermogravimetric Analysis of Gel Electrolyte. At the beginning of this work, it was contemplated that thermogravimetry may be helpful in analyzing the existence of various components in the gel. This expectation was further raised by preliminary work in the thermogravimetric (TG) and derivative thermogravimetric (DTG) curve of the individual components (HNBR, plasticizer, and LiBF_4) (Figures 19-21), which show volatilization/decomposition in distinctly different temperature ranges. However, when all the three components are together (Figure 22) only two distinct peaks are observed, with a

Sample: ZETPOL 1020 VAC DRIED
 Size: 15.0980 mg
 Method: TGA-RT-500
 Comment: 10°C/MIN, NIT. LIQ NIT GAS

TGA

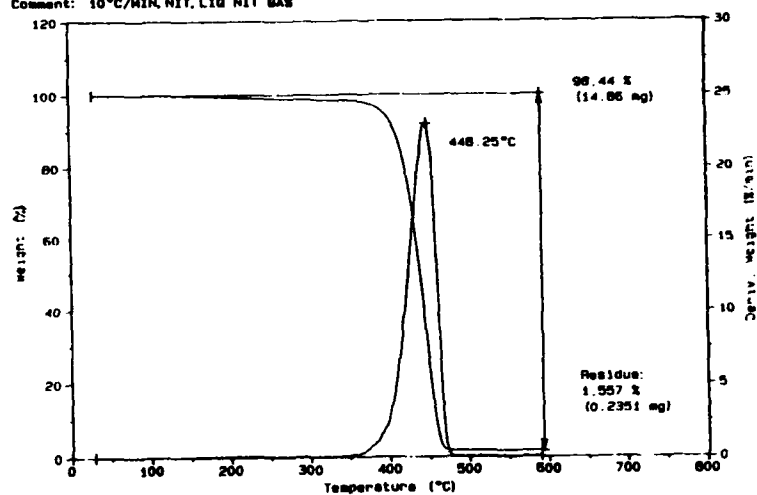


Figure 19. TG-DTG Curve of HNBR (milled).

TGA

Comment: 10°C/MIN, NIT. LIQ NIT GAS

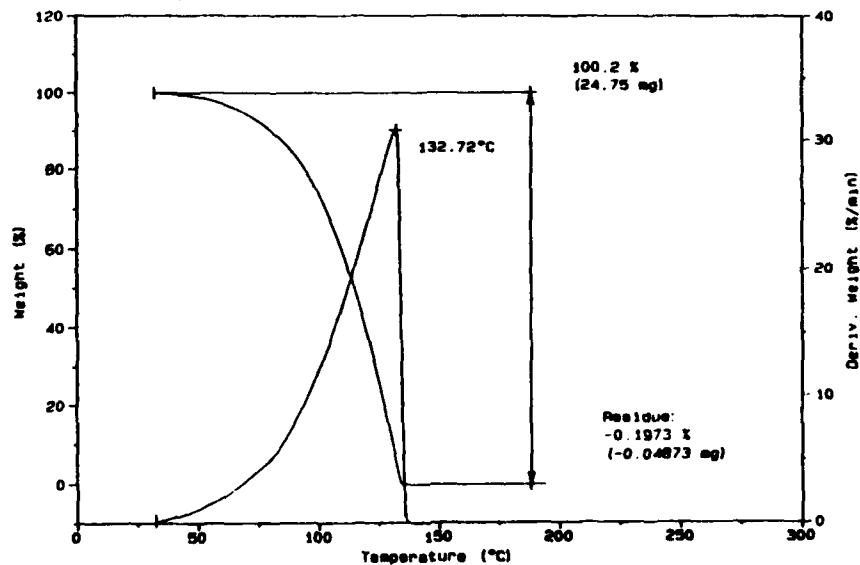


Figure 20. TG-DTG Curve of NMP.

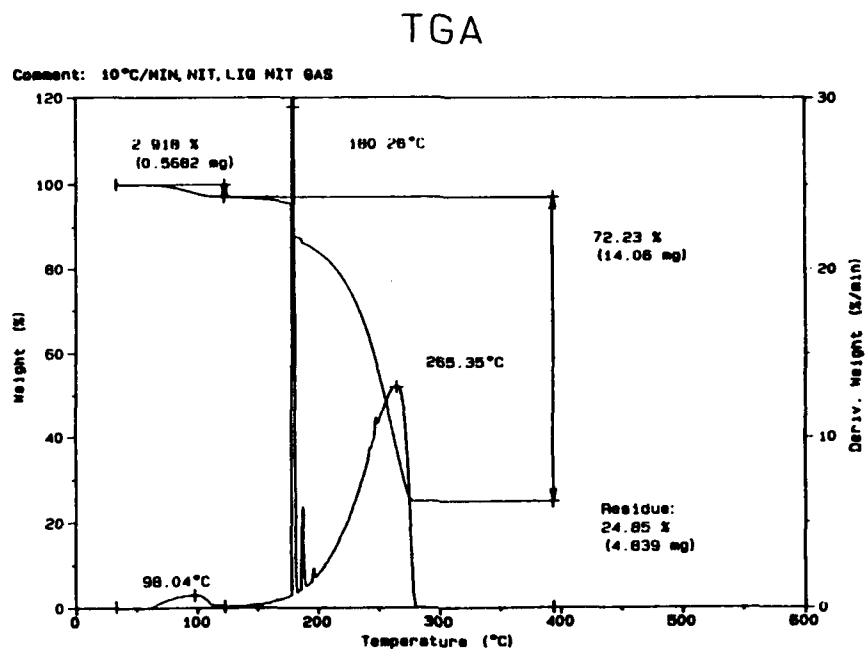


Figure 21. TG-DTG Curve of LiBF_4 .

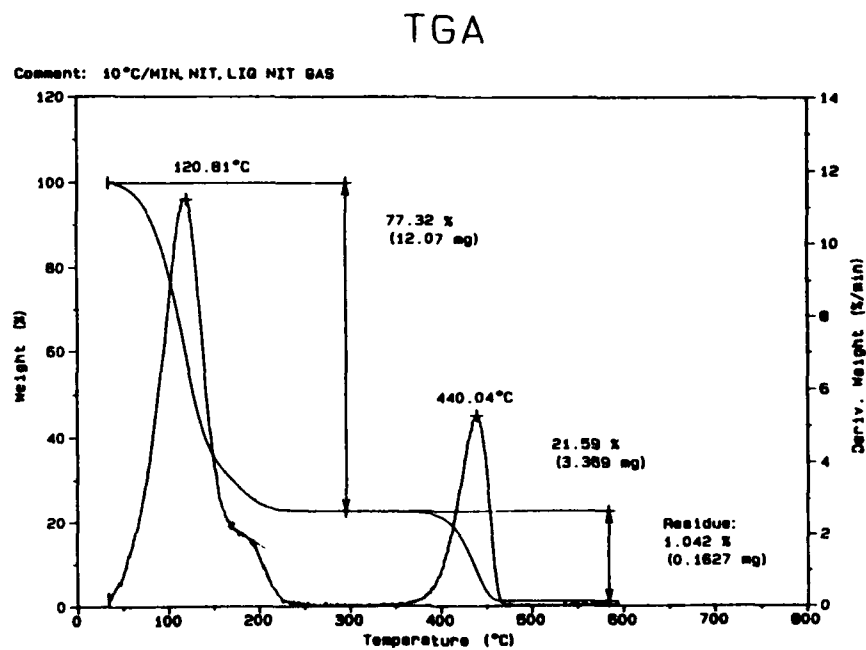


Figure 22. TG-DTG Curve of $\text{HNBR/LiBF}_4/\text{NMP}$ (15.64/6.16/78.2).

shoulder in the NMP peak around 200°C, probably indicating LiBF₄ decomposition. All the peak temperatures are lower than those of the individual components. Calculated compositions from this curve for NMP, LiBF₄ and HNBR are 70%, 8.3% (including residue) and 21.6 respectively, as compared to the known values of 78.6, 6.2 and 15.6%, respectively. Thus, TG analysis shows a lower amount of NMP and higher amount of polymer. Also, LiBF₄ shows only as a shoulder in NMP peak (incomplete separation), instead of a separate peak at higher temperature. This indicates some interaction of NMP and LiBF₄. It is possible that this interacted product decomposes along with the polymer, thus increasing the proportion attributed to the polymer.

In order to exclude the effect of any solvent, solid Zetpol 1020 and LiBF₄ were weighed directly in the TG pan (Figure 23). There is a small peak at 123°C, which may be due to absorbed water during the experiment. The other two peaks correspond to LiBF₄ (Figure 21) and HNBR (Zetpol 1020) (Figure 19) with slightly different peak temperatures. Attempts to derive the percentage composition from the TG curve shows about 27% weight (including 8.2% ash) attributed to LiBF₄ and 68.7% ascribed to polymer as compared to 34.7 and 65.3% known composition for LiBF₄ and polymer, respectively. This again indicates that a part of LiBF₄ or its decomposition product is volatilizing along with the polymer, presumably due to some interaction with the polymer and formation of a product with higher stability.

The above trend is much more apparent in cast film of HNBR/LiBF₄ in DMF (Figure 24). Here, the LiBF₄ peak is at a much lower temperature and is very flat. Again, TG determined LiBF₄ is much lower and the polymer is much higher, indicating that a part of LiBF₄ is volatilizing with the polymer.

The above study indicates that there is some interaction between LiBF₄ and NMP and LiBF₄ and HNBR, probably forming intermediate complexes that decompose at higher temperature along with the polymer. Thus, TG-DTG would not be a reliable technique to determine percent composition of this electrolyte system.

IR Studies of Gel Electrolyte. Infrared studies were carried out in order to study complexation of LiBF₄, either with the polymers or the solvents, as indicated by TG-DTG. Studies were carried out with HNBR (Zetpol 1020) and NBR (Nipol 1000X88 and 1453) in DMF and with HNBR and PAN in NMP. It was very difficult to remove last traces of solvent in the films. Vacuum drying at temperatures over 50°C causes a substantially different spectrum in the case of DMF as solvent. Therefore, prolonged air drying of the

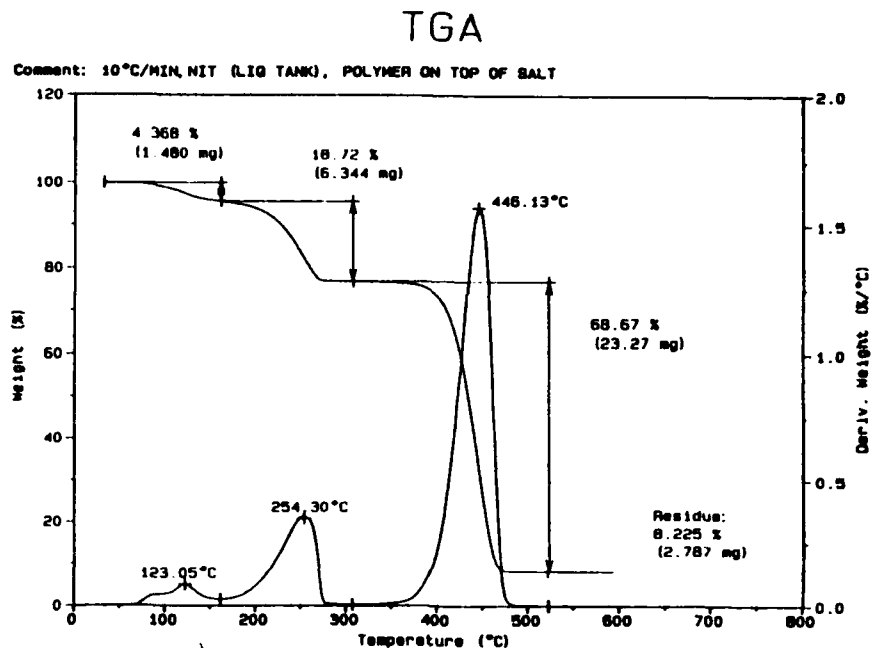


Figure 23. TG-DTG Curve of HNBR/LiBF₄ (65/35) Solids Weighed Directly into the TG Pan.

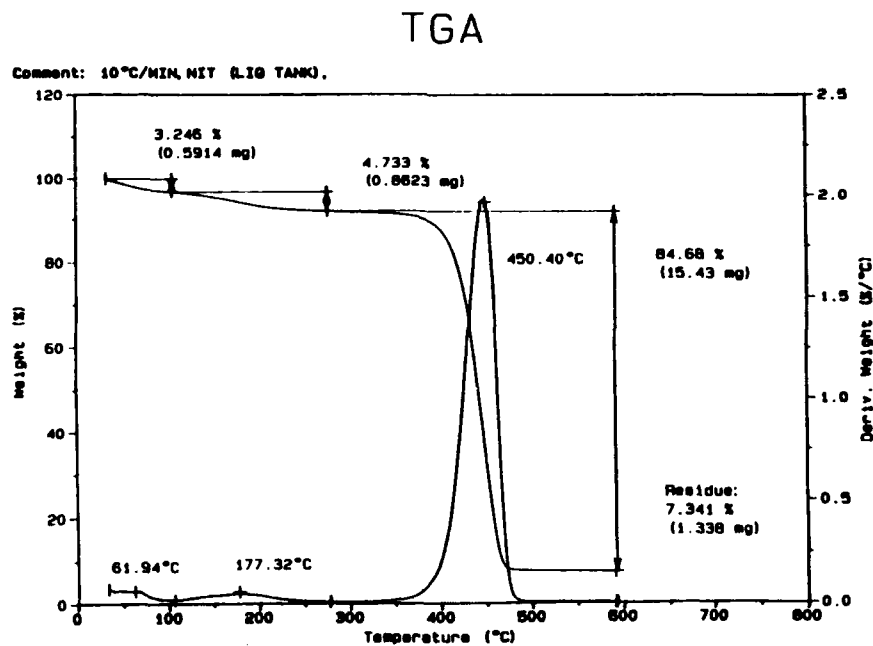


Figure 24. TG-DTG Curve of HNBR/LiBF₄ (CN/Li = 2) Cast From a DMF Solution and Dried in a Vacuum Dessicator for Three Days.

sample on a NaCl plate was carried out inside the equipment. For samples with CN:Li=2, this took 10 and 17 days for complete removal of DMF from Nipol 1000X88 and Nipol 1453, respectively. However, it was observed that leaving traces of the solvent in the sample does not alter the peak ratios (Figure 25) attributed to polymer-lithium interaction, as will be discussed later. The extra peak due to C=O vibration at 1695 cm^{-1} decreases with time of drying and is almost nonexistent after drying is complete, both for polymer with or without LiBF_4 . The peak may be attributed to lithium-DMF complex which breaks down with extended drying.

Figure 25 illustrates the magnified IR peaks for HNBR alone (lower curve) and with LiBF_4 in DMF. HNBR shows two peaks at wave numbers 2236 and 2215 cm^{-1} . An extra peak for the sample containing the lithium salt at 2262 cm^{-1} is attributed to complexation of lithium with the CN group of the polymer.

DMF shows as a single C=O peak at 1680 cm^{-1} (lower curve), whereas in presence of LiBF_4 it shows either two peaks or splitting or shoulder with an additional peak at 1695 cm^{-1} . The additional peak at 1695 cm^{-1} indicates complexation of DMF with the lithium salt. Normally, the C=O peak frequency shifting to higher wave number as a result of coordination to other species would not be expected. However, Silverstein et al.^[36], have suggested that electron-attracting groups attached the frequency of absorption to the nitrogen increase since they effectively compete with the carbonyl oxygen for the electrons of the nitrogen, thus increasing the force constant of the C=O bond. A somewhat similar situation can occur if the interaction of lithium is conceived to occur with the nitrogen atom of the tertiary amide, rather than with the carbonyl oxygen, partially immobilizing a lone pair of electrons through resonance effect. There is also other evidence to support the observation that interaction of lithium with tertiary amides (DMF, DMAC) may be through the amide nitrogen^[37].

Similar IR absorbance spectra for NBR of different unsaturation are shown in Figures 26 and 27 for Nipol 1000X88 and Nipol 1453, respectively. In contrast to HNBR, the NBR polymers do not show the peak at 2215 cm^{-1} . A single peak at 2236 cm^{-1} , attributed to CN vibrations, is observed for both polymers in the absence of the lithium salt (lower curves). However, the extra peak at 2264 cm^{-1} attributed to complexation is observed for both polymers. Also, the intensity of the 2264 cm^{-1} peak is higher for NBR with 44 percent acrylonitrile than that in NBR with 28 percent acrylonitrile (c.f. Figs. 26 and 27). Thus, IR studies of NBR and HNBR copolymers indicate complexation of CN group with lithium. However, the reason for the extra peak of HNBR at 2215 cm^{-1} is not apparent.

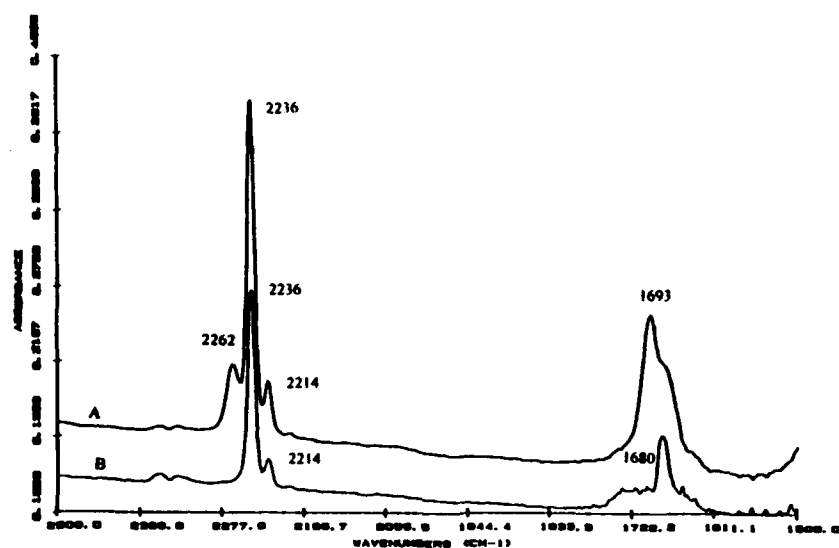


Figure 25. IR Absorbance Spectra for A) HNBR With LiBF_4 (CN/Li=4) and B) HNBR Alone.

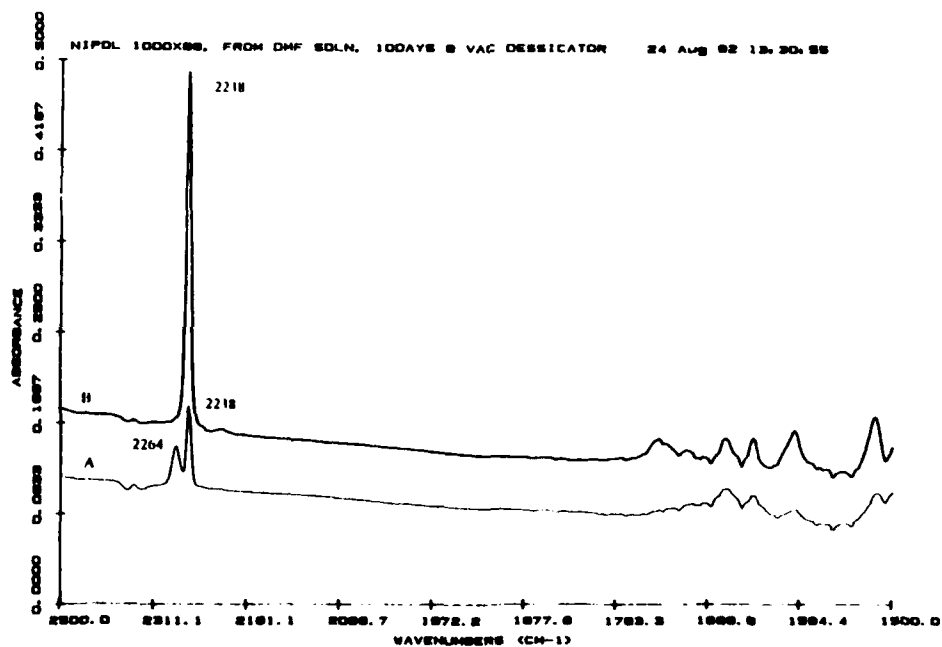


Figure 26. IR Transmission Spectra of A) NBR (44% ACN) with LiBF_4 (CN/Li=2) and B) NBR Alone. Both cast from DMF solution.

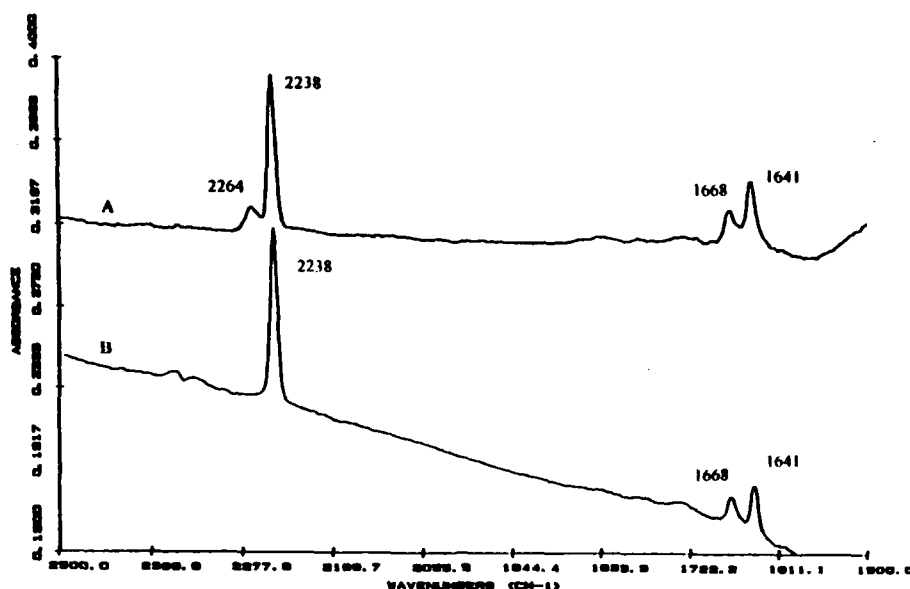


Figure 27. IR Absorbance Spectra of A) NBR (28% ACN) with LiBF_4 ($\text{CN/Li}=2$) and B) NBR (28% ACN) Alone.

Efforts were made to correlate the absorbance ratio of 2262/2236 peaks to CN:Li ratio. The data for NBR (44% AIN): $\text{LiBF}_4=1,2$, and 8 are 0.224, 0.104, and 0.082 which show a linear relationship when IR absorption ratio is plotted versus percent lithium in Li/NBR film made from DMF solution (Figure 28).

As in DMF, HNBR (Zetpol 1020) shows two peaks at 2236 and 2215 cm^{-1} assigned to CN vibrations in NMP. (HNBR + LiBF_4) also shows two CN peaks at 2236 and 2215 cm^{-1} . However, as shown in Figure 29 the additional peak at 2262 cm^{-1} attributed to the CN-Li complex is missing. Instead, broad C=O peaks attributed to complexes with NMP appears around 1646 and 1664 cm^{-1} . NMP alone shows a sharp C=O peak at 1688 cm^{-1} . The intensity of the broad peak at 1646 cm^{-1} did not decrease on further drying. (Zetpol + NMP) (Figure 30) does not show this peak, but (LiBF_4 + NMP) (Figure 31) does. All these indicate that NMP is strongly bonded to the salt, with or without involvement of HNBR, and lithium is solvated at the carbonyl group, in contrast to DMF.

In the case of PAN/ LiBF_4 /NMP, behavior similar to HNBR is observed. The C=O peak for NMP is broadened and shifted to lower wave numbers around 1660 and 1648 cm^{-1} (Figure 32), and showed no decrease with additional drying. Also, no C=O peak was

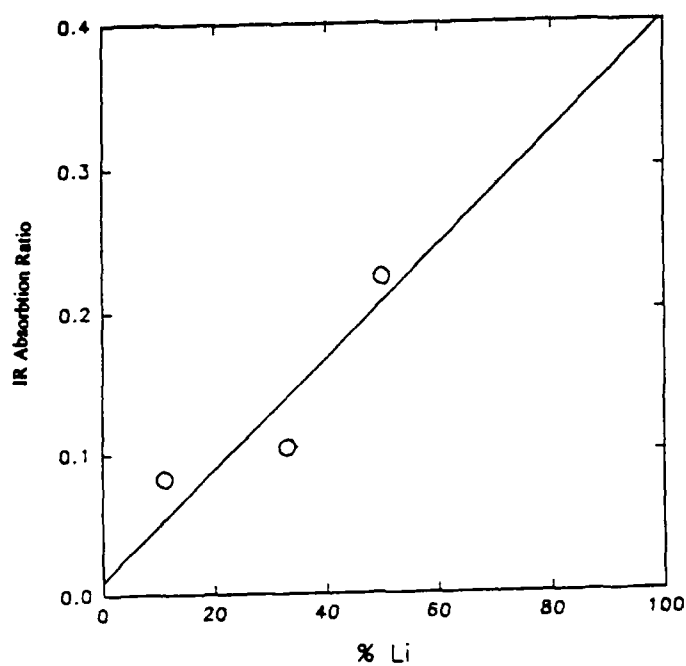


Figure 28. IR Absorbance Ratio (2262/2236 cm^{-1} vibrations) vs Percent Li in Li/NBR Film.

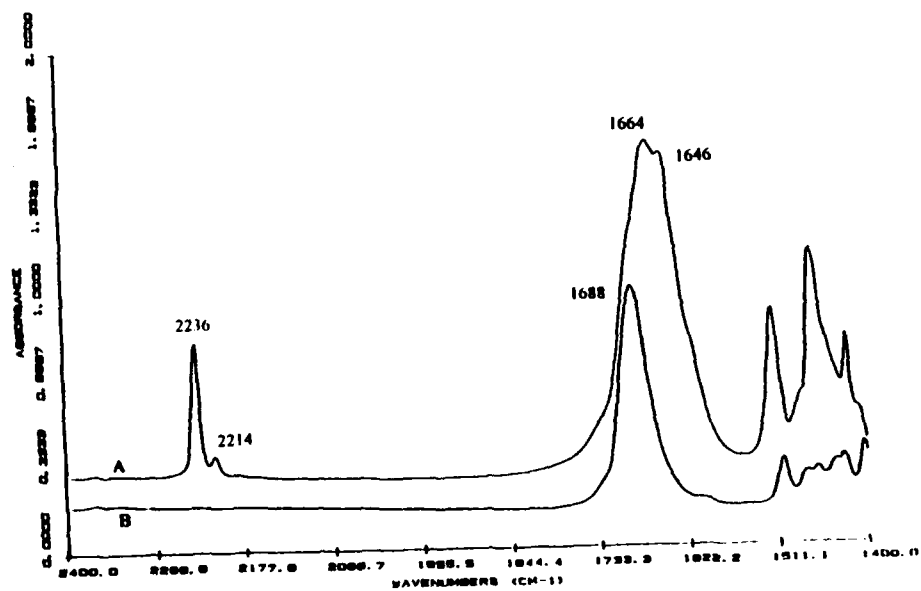


Figure 29. IR Absorbance Spectra of A) HNBR/LiBF₄/NMP Gel (CN/Li=4) and B) NMP.

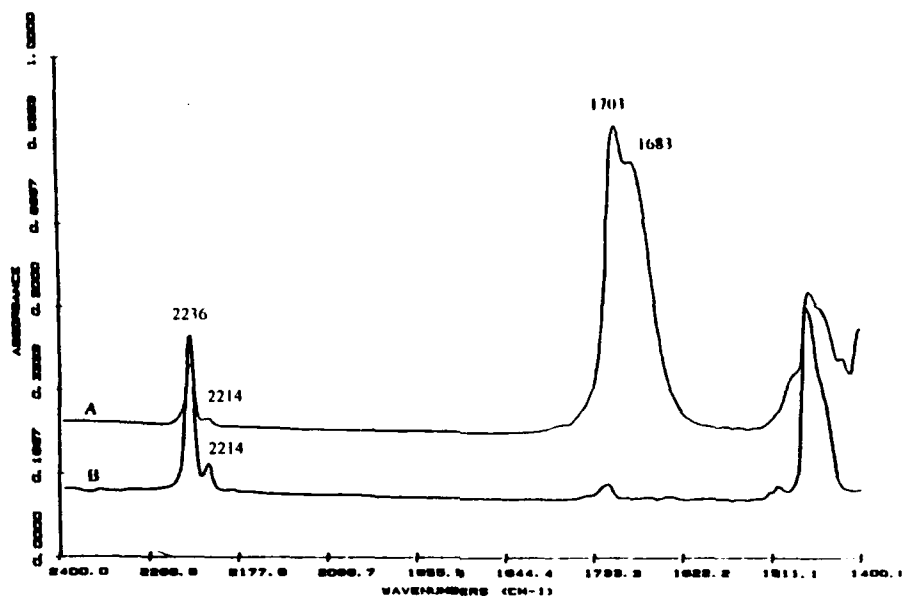


Figure 30. IR Absorbance Spectra of A) HNBR Film from NMP and B) HNBR Film from DMF.

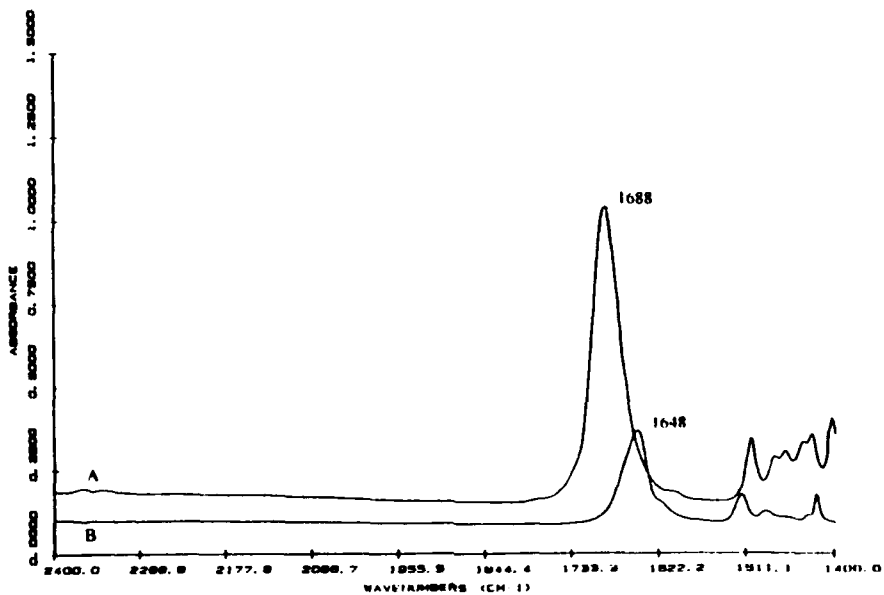


Figure 31. IR Absorbance Spectra of A) NMP and B) LiBF₄, Cast from NMP Solution.

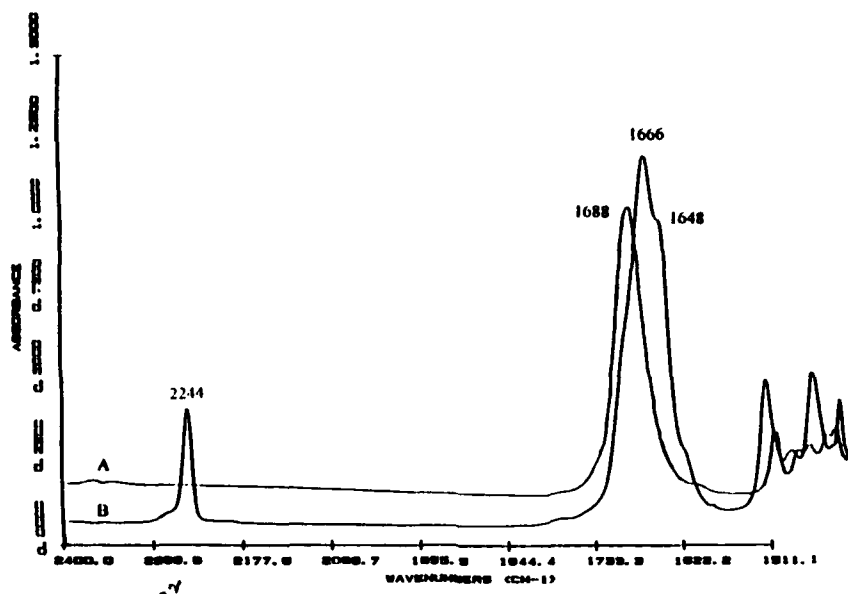


Figure 32. IR Absorbance Spectra of A) NMP and B) PAN/LiBF₄ (CN/Li=4) Film from a 3% NMP Solution.

detected in the PAN sample pressed with KBR (Figure 33). All these facts again indicate strong involvement of NMP and LiBF₄. The only difference with HNBR is that the peak at 2264 cm⁻¹ is visible as a shoulder while with HNBR (Fig. 30) it is absent.

In the case of PAN/LiBF₄/DMF, the C=O peak for DMF is broadened and shifted to lower wave numbers around 1662 and 1648 cm⁻¹ (Figure 34, curve B). There is no indication of interaction between DMF and PAN (curve A), i.e., there is no shifting or broadening of the peak. Surprisingly, the 2262 cm⁻¹ peak present both for NBR and HNBR in DMF shows only as a shoulder for PAN in both DMF and NMP (Figures 33 and 34). This is quite unexpected in view of the data in Figures 26 and 27 where the 2262 cm⁻¹ peak intensity increases with CN in the polymer, and the data indicating proportionality of CN:lithium versus IR peak absorption ratio (Figure 28). This indicates a decrease of interaction between the polymer and the salt, although PAN has a much larger number of CN groups than the copolymers. As mentioned earlier, the presence of HNBR in the hybrid film influences the conduction process raising the E_a value, in comparison to that in solution, while PAN does so only at very high concentration^[21]. This difference in interaction may result from the differences in T_g values of the two polymers.

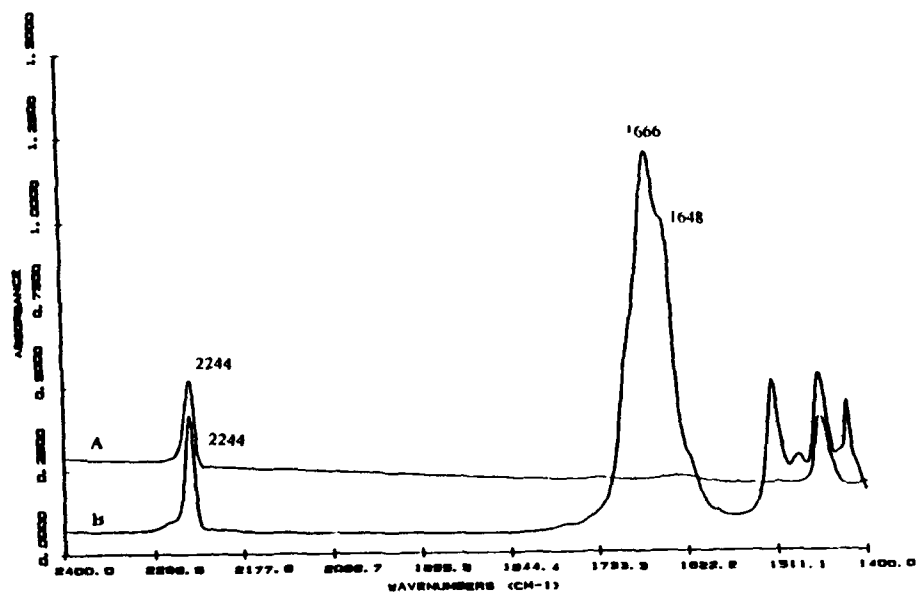


Figure 33. IR Absorbance Spectra of A) PAN in a KBr Plate and B) PAN/LiBF₄ (CN/Li=4) Film. Cast from a 3% NMP Solution and Dried for 5 Days in the IR Compartment.

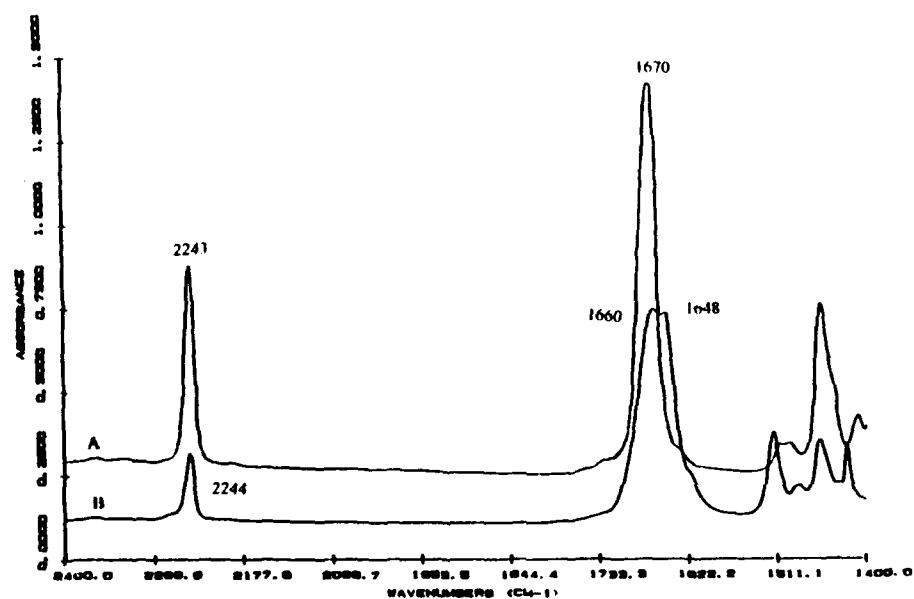


Figure 34. IR Absorbance Spectra of A) PAN Film, Cast from a DMF Solution and Dried for 2 Days and B) PAN/LiBF₄ (CN/Li=4) Film, Cast from a 3% DMF Solution and Dried for 3.5 Days.

The above observations raise the question as to the desirability of Li/polymer interaction in promoting conductivity of the hybrid films. However, the answer to this question is beyond the scope of this investigation.

Efforts were made to determine the involvement of the -C=C- bond in the butadiene part of NBR in complexing with Li^+ . Two types of absorption are due to unsaturation in polybutadienes. The out of plane =C-H bending is usually strongest in the spectra of alkanes; C=C stretching is usually weak. The wave numbers for the bending and stretching vibrations vary according to trans-1,4-, cis-1,4; and sidechain (1,2) structures and are 970 and 1670 cm^{-1} for trans-1,4; 730 and 1650 cm^{-1} for cis-1,4; and 990 and 1640 cm^{-1} for side chain 1,2 structures. Figure 35 shows no shift of any of these peaks, with and without LiBF_4 in the case of NBR films with 44 percent ACN (1000X88), prepared from DMF solutions. This indicates none or little involvement of double bonds in complexing with Li^+ .

Cyclic Voltametry. Attempts were made to measure the electrochemical stability window of the hybrid films made of Zetpol 1020/NMP/ LiBF_4 . However, the lithium electrode is immediately attacked by NMP and it turns black. It was observed that NMP turns yellow when a lithium foil is dipped into it. Figure 36 shows the cyclic voltametry curve which indicates poor stability of the electrodes.

The IR study conclusively show strong interaction of LiBF_4 with NMP. The lack of interaction of LiBF_4 with the polymers in presence of NMP indicate that lithium preferentially bonds with NMP, with little involvement with the polymer. On the other hand, both NBR and HNBR complex with lithium when made in DMF, but PAN shows very little interaction.

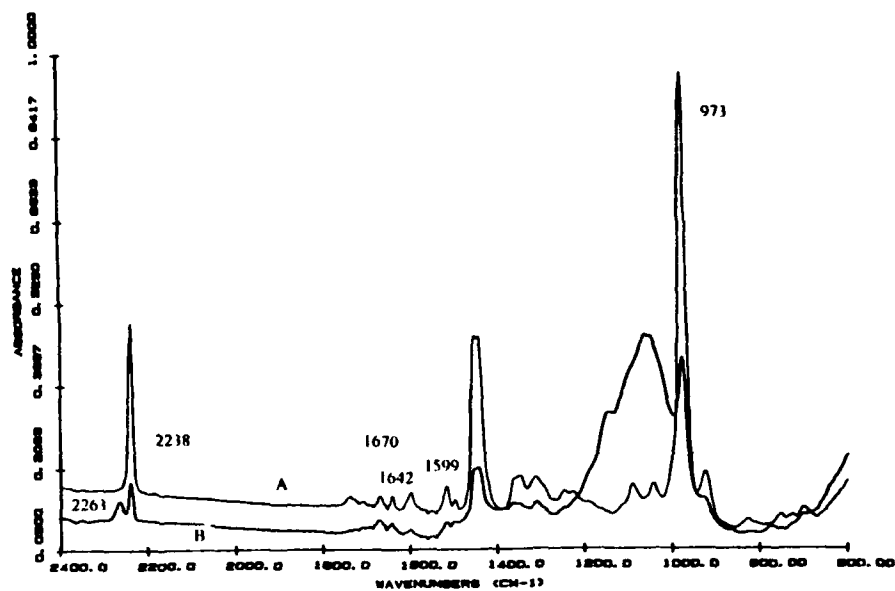


Figure 35. IR Absorbance Spectra of A) NBR (44 percent ACN), Cast from DMF Solution and B) NBR (44 percent ACN/LiBF₄, Cast from a 5 percent DMF Solution and Dried 10 Days in IR Compartment.

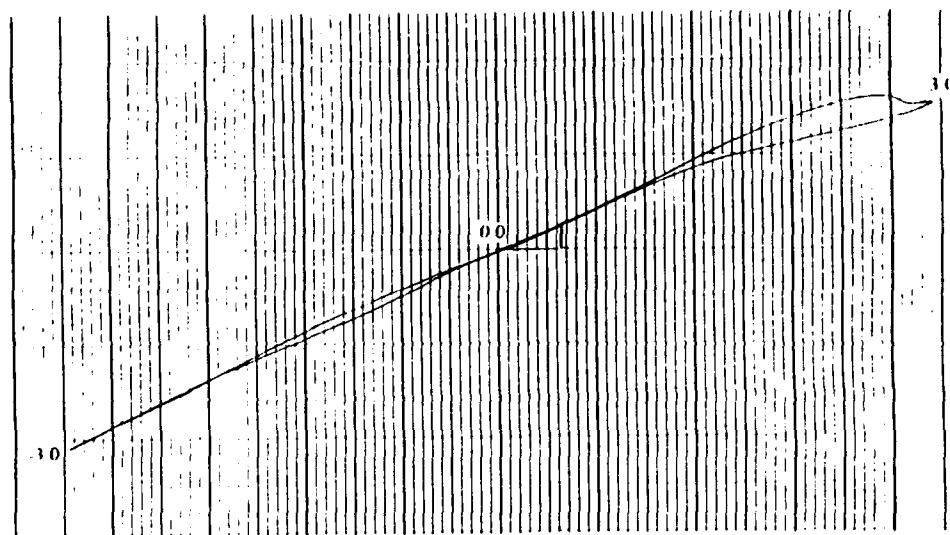


Figure 36. Cyclic Voltammogram for 10 percent LiBF₄ in NMP with a Lithium Working Electrode and a Lithium Reference Electrode (20 mV/s, ± 3.00 Vdc).

5. SUMMARY AND CONCLUSIONS

This study is concerned with the preparation of a hybrid electrolyte, suitable for solid-polymer batteries. Based on the study of electrical conductivity in the presence of LiBF_4 of a number of nitrile-butadiene copolymers (NBR), (presented in Appendix B), a hydrogenated NBR (HNBR) was selected as the host polymer. DC conductivity studies with three different lithium salts in different plasticizers showed the highest conductivity for LiBF_4 . Conductivity of LiBF_4 in different plasticizers decreases in the order $\text{DMF} > \text{DMAC} > \gamma\text{-butyrolactone} > \text{NMP} > \text{PC} = \gamma\text{-valerolactone} > \text{glymes}$. NMP was chosen as the plasticizer for hybrid films based on its moderate conductivity, low vapor pressure, and low freezing point.

Ionic conductivity was determined both in homogeneous solution of the components (DC conductivity) and in hybrid films (by impedance). Maximum DC conductivity is observed with a maximum critical concentration of LiBF_4 , which varies in different plasticizers. For NMP it is about 8 percent LiBF_4 by weight. Maximum achieved conductivities in solution are 2.2×10^{-2} , 1.6×10^{-2} , 9.2×10^{-3} , 8.8×10^{-3} , 4.9×10^{-3} , 4.9×10^{-3} , and 4.9×10^{-3} for DMF, DMAC, NMP, γ -butyrolactone, γ -valerolactone, and propylene carbonate, respectively. For solutions with polymer, conductivity decreases as CN:Li increases. Although conductivity decreases in the presence of the polymer, the E_a remains unaltered at approximately 0.11 eV/mol, provided all components are in solution. Also, the energy of activation is the same for all plasticizers studied, although absolute values of conductivity are different.

An opposite relationship of conductivity with polymer/lithium ratio was observed for the hybrid films. Here conductivity decreases as the polymer/lithium ratio decreases. This may be caused by decreased mobility due to tremendous increase of viscosity, as the lithium concentration increases at low CN:Li.

In the hybrid film, conductivity increases as the plasticizer to salt ratio increases. Plasticizer to salt ratio has a larger effect than the polymer:lithium ratio. The highest conductivity observed is around 3.5×10^{-4} S/cm for 4:1:8.7, HNBR:Li:NMP as compared to 2.5×10^{-3} for homogeneous solutions with polymer at the same polymer:Li ratios and 5.8×10^{-3} for 2.5 percent LiBF_4 in NMP. The energy of activation for the hybrid film is much higher than in solution (0.31 eV/mol vs 0.11 eV/mol). The higher E_a for the hybrid films is attributed to the additional energy necessary to overcome the resistance at the solid/liquid interface and ionic transport through the plasticized solid polymer.

Higher conductivity might be possible with high solvent/salt ratio at the expense of inferior mechanical properties. However, these polymers can be easily cross-linked to improve mechanical properties. A desirable feature of these films is the good adhesion to the electrodes. Thermogravimetry and IR data indicate considerable interaction of NMP with LiBF_4 .

It may be concluded that the system HNBR/ LiBF_4 /NMP is rather complex. There is not only an interaction of HNBR and lithium, but also an additional interaction with NMP.

6. RECOMMENDATIONS

Although this work did not produce a practical film for solid-state batteries, a number of worthwhile observations were made. A workable film can however be made based on this study, as explained below. Shortage of time did not allow us to implement these solutions.

- It is obvious, that NMP should be replaced with another plasticizer. As shown in Figures 4 and 9, γ -valerolactone has about the same conductivity as PC. It is expected to have lower interaction with lithium. A mixture of solvents, as shown in Table 7, may also be useful to increase conductivity.
- Electrochemical stability with a new solvent should be determined at the beginning of any new study, rather than at the end.
- Since the electrical conductivity in a gel electrolyte depends on the solvent/salt ratio, a larger amount of solvent in the hybrid film would favor higher conductivity. This could not be done in the present study because of the low viscosity imparted by higher solvent/polymer ratio. If the polymer is lightly cross-linked it will be able to contain much more solvent without significant deterioration of physical properties. A desirable feature of HNBR is that it is easily cross-linked with peroxides, and does not require special techniques, such as UV irradiation.

REFERENCES

1. P.M. Blonsky, D.E. Shriver, P. Austin, and H.R. Allcock, *J. Am. Chem. Soc.* **106**, 6854 (1984).
2. M. Armand, W. Gorecki, and R. Andreani, Second Intl. Symposium of Polymer Electrolytes, Siena, Italy, (June 1989).
3. I.E. Kelly, J.R. Owen, and B.C.H. Steele, *J. Power Sources* **14**, 13 (1985).
4. M.Z.A. Munshi, and B.B. Owens, *Solid State Ionics* **26**, 41 (1988).
5. D.G.H. Ballard, P. Cheshire, T.S. Mann, and Przeworski, *Macromolecules* **23**, 1256 (1990).
6. H. Yang, R. Huq, and G.C. Farrington, 7th Int'l. Conf. on Solid State Ionics, p. 7, A-24 (Nov 1989).
7. R. Huq, R. Koksang, P.E. Tonder, and G.C. Farrington, *Proc. Electrochem. Soc. (Symp. Primary and Secondary Lithium Batteries)*, 91-93 (1991).
8. M.L. Caplan, E.A. Ritman, and R.J. Cava, *Polymer* **30**, 504 (1989).
9. J.S. Foos and S.M. Erker, *J. Electrochem. Soc.* **134**, 1724 (1987).
10. S. Tado, and H. Kawahara, *J. Electrochem. Soc.* **135**, 1728 (1988).
11. M. Alamgir, R.K. Reynolds, and K.M. Abraham, in Materials and Processes for Lithium Batteries, K.M. Abraham and B.B. Owens, ed. The Electrochem. Soc., Pennington NJ, pp. 321 (1989).
12. M. Armand and F. El. Kadiri, in Lithium Batteries, ed. A.N. Dey, The Electrochem. Soc., Pennington, NJ. pp. 502 (1987).
13. A. Bouridah, F. Dalard, D. Deroo, H. Cheradaine, and J.F. LeNest, *Solid State Ionics* **15**, 233 (1985).
14. E. Kronfli, K.V. Lowell, A. Hooper, and R.J. Neat, *Brit. Polym. J.* **20**, 275 (1988).
15. R. Koksang, F. Flemming, I.I. Olsen, P.E. Tonder, K. Brondum, M. Consigney, K.P. Petersen, and S. Yde-Anderson, *Proc. Electrochem. Soc. (Symp. Primary and Secondary Lithium Batteries)* 91-3, pp. 157-169 (1991).
16. M. Gauthier, D. Fauteux, G. Vassort, A. Belanger, Ricoux P. Duval, J.M. Gabano, D. Muller, P. Rigaud, M.B. Armand, and D. Deroo, *J. Electrochem. Soc.* **132**, 1333 (1985).

17. M. Alamgir, R.D. Moulton, and K.M. Abraham, Proc Electrochem. Soc (Symp. Primary and Secondary Batteries) 91-3, pp. 131-141 (1991).
18. M. Watanabe, M. Kanba, K. Nagaoka, and I. Shinohara, J. Polym. Sci., Polym. Phys. Ed. 21, 939 (1983).
19. K.M. Abraham, and M. Alamgir, J. Electrochem. Soc. 136, 1657 (1990).
20. M. Watanabe, M. Kanba, N. Natsuda, K. Tsunemi, K. Mizoguchi, K., E. Tsuchida, and I. Shinohara, Macromol. Chem., Rapid Comm. 2, 741 (1981).
21. M. Watanabe, M. Kanba, K. Nagaoka, and I. Shinohara, J. Polym. Sci., Polym. Phys. Ed. 21, 939 (1983).
22. K. Tsunemi, H. Ohno, and E. Tsuchida, Electrochem. Acta 28, 833 (1983).
23. A. Hooper, R.J. Powell, T.J. Marshall, and R.J. Neat, J. Power Sources 27, 3 (1989).
24. J.S. Lundsguard, S. Yde-Andersen, R. Koksang, D.R. Shackle, P. Austin, and D. Fauteux, 2nd Int'l. Symp. on Polymer Electrolytes, Siena, Italy (June 1989).
25. R. Koksang, I.I. Olsen, P.E. Tonder, N. Knudsen, Lundsguard, J.S. Lundsguard, and S. Yde-Andersen, J. Power Sources 32, 175 (1990).
26. P.S.S. Prasad, B.B. Owens, W.H. Smyrl, A. Selvaggi, and B. Scrosati, Proc. Electrochem. Soc. (Primary and Secondary Batteries), 91-3, 170 (1991).
27. K.M. Abraham, and M. Alamgir, 6th Int'l. Meeting on Lithium Batteries, Munster, Germany (May 10-15, 1992).
28. F.M. Gray, In Polymer Electrolyte Reviews -1 (J.R. MacCallum and C.A. Vincent, eds.), Elsevier Applied Science, New York, 1987.
29. S. Reich and I. Michaeli, J. Polym. Sci., Polym. Phys. Ed. 13, 9 (1975).
30. E. Tsuchida, H. Ohno, and K. Tsunemi, Electrochim. Acta 28, 591 (1983).
31. M.B. Armand, Solid State Batteries, (C.A.C. Sequeira and A. Hooper, eds.) NATO ASI Series, Martinus Nijhoff, Dordrecht (1985).
32. K.S. Cole and R.H. Cole, J. Chem. Phys. 9, 341 (1941).
33. J.R. McDonald, J. Chem. Phys. 58, 4982 (1973).
34. A. Tranchant, N. Lebrun, and R. Messina, 6th Int'l. Meeting on Lithium Batteries, Munster, Germany, (May 10-15, 1992).
35. T. Miyamoto and K. Shibayama, J. Appl. Phys. 44, 5372 (1973).

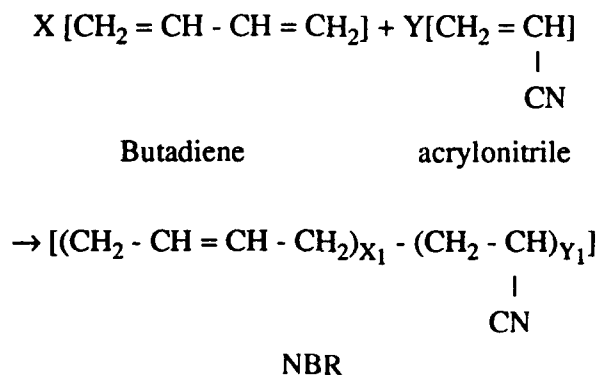
36. A.M. Silverstein, G. Barsler, and T.C. Morrill, in Spectrometric Identification of Organic Compounds, 5th Ed., John Wiley & Sons, New York.
37. L.G. Scanlan, presented at the Spring Meeting of the Electrochemical Society, Honolulu, HI, 16-21 May 1993.

APPENDIX A

GLASS TRANSITION TEMPERATURE OF VARIOUS NBR COPOLYMERS WITH AND WITHOUT LiBF₄

INTRODUCTION

The host polymer for the hybrid films in this study was selected from a preliminary screening of the acrylonitrile-butadiene copolymers (NBR), represented by the empirical formula:



X, X₁, Y, Y₁ are different, since the proportion of monomers in the copolymer is not directly proportional to that in the feed. The properties of the copolymers, such as oil resistance, tensile strength, and glass transition temperature (T_g) depends on the proportion of the two components in the copolymer. Commercially-available NBR copolymers range in content from 15 to 50 percent. The higher the acrylonitrile content, the higher the oil resistance and T_g. Literature data indicates that the T_g of many polymers used as polymeric electrolytes increases as it solvates lithium^[1-5]. Since electrical conductivity is greatly reduced below T_g, a study of the T_g dependence of of NBR copolymer in the presence and absence of lithium tetrafluoroborate (used as dopant) was undertaken. Peculiarities in the T_g of NBR copolymers and their causes are discussed. The advantages of the derivative DSC (DDSC) method to locate the T_g of these polymers is emphasized.

EXPERIMENTAL

The nitrile-butadiene copolymers (NBR) used were commercial elastomers obtained from Zeon Chemical Corporation. The bound acrylonitrile aimed during manufacture, given in parenthesis, are as follows: Nipol 1000X132 (50.5), Nipol 1000X88 (43.9), Nipol 1401LG (40.9), Nipol 1042 (33), Nipol 1453HM (28.3), Nipol 1034-60 (20.3). In addition, Zetpol 1020, a hydrogenated NBR copolymer (HNBR) with the same acrylonitrile content as Nipol 1000X88

(43.9) with about 10% of the original unsaturation unreacted and saturated polymer polyacrylonitrile (PAN), were used. The polymers were used as-received after vacuum drying at 60°C for 24 hours. The samples with and without lithium tetrafluoroborate (LiBF_4) were cast from the 3 percent polymer solution in corresponding solvents and dried for 2 days in vacuum to obtain a film with the desired amounts of the components. Clear solutions were obtained in DMF for all the polymers except 1000X132 and 1034-60. The latter is soluble in MEK. The NBR: LiBF_4 films are very hygroscopic and were preserved inside a vacuum dessicator.

T_g Measurements

TA Instruments 2910 DSC under nitrogen purge and a heating rate of 10°C/min was used for the T_g measurements. Low temperature calibration of the instrument at the same heating rate was carried out with cyclohexane (65°C and -83°C). The samples were annealed at 100°C for 5 min and quenched (30°C/min) with liquid nitrogen to -100°C. It was equilibrated at 100°C for 5 min before starting the run.

Since there are different procedures for locating the T_g ^[6], both "extrapolated onset" and the "midpoint" temperature are reported as T_g in this work, following the ASTM procedure. The former is defined as the temperature at the cross section of the extrapolated baseline and tangent of the maximum slope. The latter is the temperature at half-height of the T_g transition. The derivative DSC (DDSC) curves are also shown in the figures and are discussed in the text.

RESULTS AND DISCUSSION

Although this study was undertaken to determine the effect of the lithium tetrafluoroborate on the T_g of NBR copolymers, the authors came across several interesting observations which may have implications on the method of T_g determination in NBR or other similar copolymers. These are discussed briefly in the following paragraphs before going into the effect of LiBF_4 on T_g .

Peculiarities in the T_g Curves of NBR Copolymers

Generally, T_g s of the random copolymers are intermediate to those of the components and depends on the proportion of the constituent monomeric units. This is also true for NBR copolymers^[7]. As the proportion of acrylonitrile in the copolymer increases, T_g increases. This is evident in Table A-1. However, below 36% acrylonitrile the NBR copolymers have two T_g s. This has been reported previously^[8-11] and was attributed to the different distribution of acrylonitrile and butadiene in high- and low-nitrile NBR copolymers. The reactivity ratios of

TABLE A-1
Glass Transition Temperature of NBR Copolymers

Trade Name	Bound ACN %	Extrapolated Onset		Midpoint		DDSC	
		T _{g1}	T _{g2}	T _{g1}	T _{g2}	T _{g1}	T _{g2}
Nipol 1000X132	50.5	-14	---	-9.9	---	-9.4	---
Nipol 1000X88	43.9	-15.7	---	-13.0	---	-11.7	---
Nipol 1401LG	40.9	-20.6	---	-17.8	---	-15.2	---
Nipol 1042	33.0	-32.9		-21.6		-26.1	-16.8
Nipol 1453HM	28.3	-52.4	-26.7	-49.0	-24.0	-50.0	-25.5
Nipol 1034.60	20.3	-68.3	-30.7	-63.9	-27.6	-63.7	-28.1
Nipol 1432 ^a	33.0	-41.8	-24.3			-18.3	
Zetpol 1020 ^b	44.0	-21.1		-18.3			

^a Contains >20% vinyl acetate-vinylchloride copolymer (VYHH)

^b Hydrogenated NBR residual unsaturation 10%

acrylonitrile and butadiene monomers are both very much less than unity^[12]. Consequently, at a high acrylonitrile charge ratio there is a strong tendency for the growing chain to alternate between the addition of acrylonitrile and butadiene monomers^[13]. On the other hand, at a low acrylonitrile charge ratio (25/75, acrylonitrile/butadiene), the composition of the polymer depends on the degree of conversion. Alteration of both monomers is favored up to a 40 percent degree of conversion, producing a polymer comparatively richer in acrylonitrile (~35 percent) than the charge. The initial depletion of acrylonitrile causes the polymer formed at higher conversion to be rich in butadiene. Thus, for the NBR polymers with less than 36 percent ACN there are two polymeric phases which gives rise to two T_gs. This is illustrated in Figures A-1 and A-2 for NBR copolymers with 44 percent (single T_g) and 20 percent (two T_gs) ACN, respectively. Polymers with two T_gs, are designated T_{g1} and T_{g2} for the high and low temperature transitions, respectively, in Table A-1.

From the explanation of the two-phase systems as above, it would be expected that as the nitrile content of NBR increases from 20 to 35 percent the composition of the phases will get closer to each other. This will diminish the difference of T_{g1} and T_{g2} (ΔT_g). Landi^[14] observed that the temperature difference between transitions and the relative intensity of the smaller low

Sample: NIPOL 1000x88
 Size: 5.2670 mg
 Method: COND. POLYM.
 Comment: 10°C/MIN, CAST FROM 2% SOLN IN DMF

DSC

File: NDSC0839.01
 Operator: GALASKA
 Run Date: 20-Nov-92 15:00

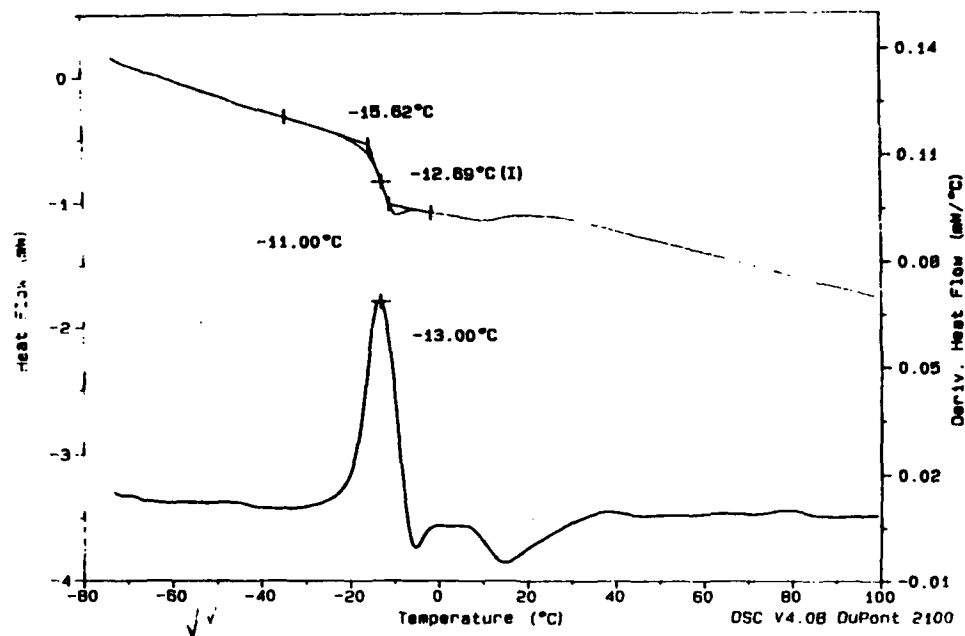


Figure A-1. Glass Transition Temperature of NBR Copolymer (Nipol 1000X88) with 44 percent ACN.

Sample: NIPOL 1034-60 milled
 Size: 8.4610 mg
 Method: DSC-COND
 Comment: 10°C/MIN, N2

DSC

File: NDSC0538.01
 Operator: GALASKA
 Run Date: 9-Apr-92 12:39

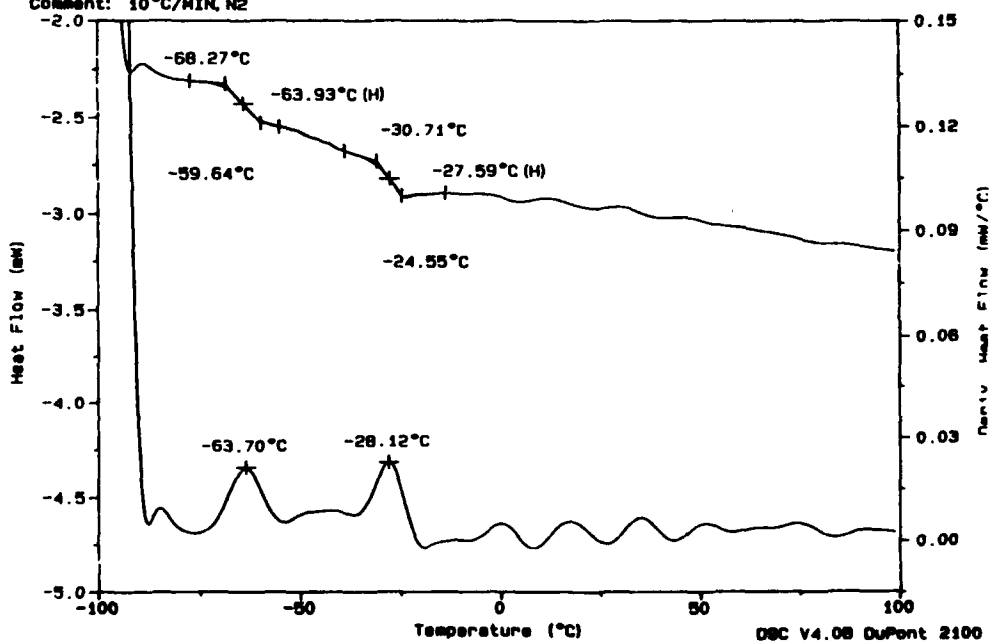


Figure A-2. Glass Transition Temperature of NBR Copolymer (Nipol 1034-60) with 20 percent ACN.

temperature transition both become greater at lower nitrile content. This is shown very nicely in the ΔT_g vs nitrile content in Figure A-3. However, Figure A-3 indicates the ΔT_g should be equal to zero at about 36 percent ACN which is the azeotropic composition of butadiene and acrylonitrile monomers for reaction at 50°C^[14].

Assignment of T_g

Although T_g has been used for characterization of polymers for a long time, there is some confusion in the literature as to the location of T_g . Both the extrapolated onset and the midpoint of inflection (as shown in Figures A-1 and A-2) have been recommended by ASTM D3418. However, the T_g value would be different depending on the location selected. It may be pointed out that, in contrast to thermoplastics where the extrapolated onset is the temperature where the first indication of the loss of useful property (i.e., softening) is manifested, the opposite is true for the elastomers. Here, the loss of elastomeric properties is indicated earlier (at higher temperature) in the transition region as the sample is cooled and at the extrapolated onset the elastomeric chains are at close proximity to the glassy state.

Use of Derivative DSC

The DDSC curves shown in Figures A-1 and A-2 offer another alternative to locate T_g . These curves exhibit a peak corresponding to the maximum rate of change of slope of the endothermic shift accompanying T_g . As shown in Table A-1, the DDSC peaks more or less coincide with the midpoint value of the T_g shift, thus facilitating its location. Landi^[14] reported DDSC curves for a series of NBR elastomers. Another advantage of DDSC curves which is not mentioned in the literature is shown in Figure A-4 for T_g of NBR with 33 percent ACN. This elastomer has ACN composition which is in the borderline of NBRs having one or two T_g s. Similar elastomers have T_g s at -32°C and -24°C T_g s at a heating rate of 10°C/min^[9]. As shown in Figure A-4, the DSC transition show only one transition. However, the broadness of the transition indicates phase heterogeneity that may be caused by two glass transitions at close proximity. This is borne out by the DDSC curve which does show two transitions at -26.1 and -17.1°C ($\Delta T_g=9^\circ\text{C}$). Evidently, the T_g located at half height of the DSC transition is an average of these two transitions and fails to give a true picture of the phase morphology. T_g values are different from the literature value, presumably because of different locations (onset vs midpoint). In contrast to these data, Landi^[14] obtained a single T_g for the 34 percent ACN copolymer by DDSC. This may be caused by (a) a difference in the percent degree of conversion between the two polymers, (b) a difference in feeding the monomers for reaction, and (c) greater sensitivity and resolution of modern DSC instruments.

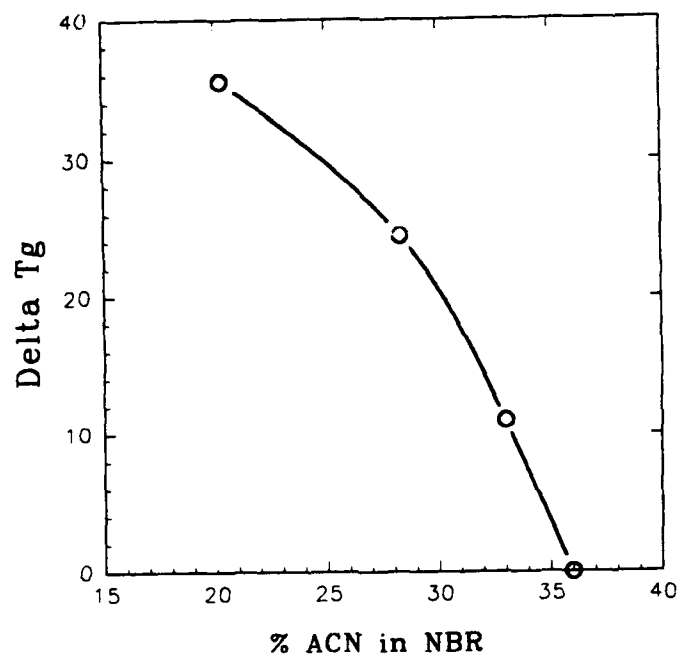


Figure A-3. Relationship Between ΔT_g vs Percent ACN in NBR Copolymers.

Sample: NIPOL 1042
 Size: 5.6310 mg
 Method: DSC W/ANNEAL
 Comment: 10°C/MIN, NIT

DSC

File: RUSC1060.01
 Operator: SALASKA
 Run Date: 6-May-93 16:57

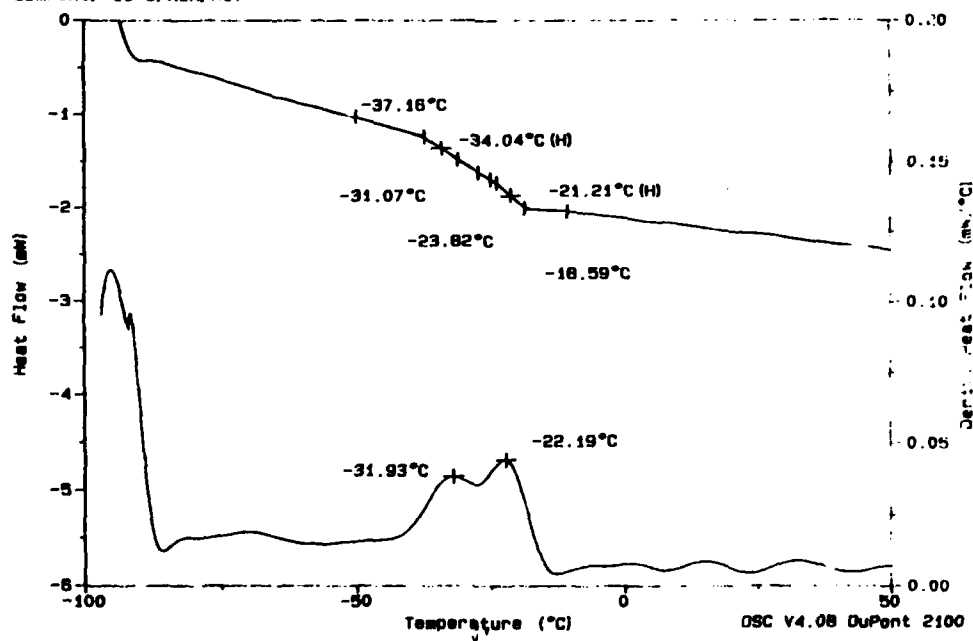


Figure A-4. DSC T_g of NBR copolymer (Nipol 1042) with 35% ACN.

Another question is whether the area under the DDSC peaks relates to the amount of different phases present in the copolymer. Preliminary experiments show this to be true, which should have an impact on quantitative determination of elastomers in compounds and vulcanizations including blend composition.

Effect of Lithium Salt on T_g

It may be observed in Table A-2 that for all NBRs over 35 percent ACN, T_g decreases when the films contain lithium tetrafluoroborate. Below 35 percent ACN, no clear trend is observed. The decrease of T_g in the presence of the lithium salt is in sharp contrast with previous work with segmented polyurethane polymer combining polyethylene oxide (PPO) soft segments^[1-4], where about 100°C increase of T_g of PPO segments was observed. This provides clear evidence for the selective dissolution of LiClO_4 in the PPO phase. Watanabe et al.^[5] observed that the salts producing the largest increase in T_g also gave complexes with higher conductivities than those showing weaker interactions, indicated by lower T_g . This is ascribed to the solvation of lithium salts to produce free ions which increases conductivity but tends to increase T_g by immobilization of chain segments. The effect of lithium salts on T_g of PEO is similar. An ionic-cross-link network is assumed where the cross-link density increases with salt concentration. Lenest^[15] observed a linear relationship between lithium perchlorate concentration versus reciprocal T_g . Thus, the overwhelming evidence in the literature is toward an increase in T_g with the addition of lithium salts.

The reduced T_g in the presence of lithium tetrafluoroborate indicates increased free volume. This can be explained by assuming that the polar interaction between nitrile groups is reduced by complexing with lithium, thus reducing intermolecular attraction of the polymer chains. This should promote segmental mobility at a lower temperature. There is not enough solvated lithium to form a network of ionic cross-links which would have increased T_g . IR data (not included here) also indicates some interaction of the nitrile group in the presence of lithium but it is rather weak in the presence of some solvents (e.g., NMP) which itself interacts with lithium.

TABLE A-2

Glass Transition Temperatures of Various NBR Copolymers
 With or Without lithium Tetrafluoroborate
 (CN:Li, 8:1, Rate of Heating 10°C/min)

Trade Name	Bound ACN %	Elastomer		Elastomer+LiBF ₄		Increase or Decrease of Tg with LiBF ₄
		T _{g1}	T _{g2}	T _{g1}	T _{g2}	
PAN	100	150.4		147		Decrease
Nipol 1000X132	50.5	-12.2		-14.0		Decrease
Nipol 1000X88	43.9	-16.4		-17.7		Decrease
Nipol 14011G	40.9	-20.6		-22.8		Decrease
Nipol 1042	33.0	-33.7				
Nipol 1453HM	28.3	-26.7	-52.4	-27.9	-52.1	Both
Nipol 1034-60 ^a	20.3	-30.7	-68.3	-26.5	-65.6	Increase
Nipol 1432 ^b	33.0	-24.3	-41.8	-20.3	-45.1	Both
Zetpol 1020 ^{c,d}	44.0	-22.8		-25.9		Decrease

^a Polymer was milled, but the solution was milky, indicating incomplete solution.

^b Contains >20% VYHH (Vinyl acetate-Vinyl chloride copolymers).

^c Hydrogenated NBR, unsaturation 10%.

^d 2=1, CN:Li.

SUMMARY AND CONCLUSIONS

The composition dependence of single or double T_g s in NBR copolymers as well as the extent of separation of two T_g s are attributed to different phases and phase compositions. As the acrylonitrile content in the copolymer increases, two T_g s get closer to each other, becoming a single T_g over 35 percent acrylonitrile. Derivative DSC offers a good method to detect and identify the T_g s.

In contrast to other polymer electrolytes (PEO, PPO) where T_g increases with the addition of LiBF_4 , a small decrease of T_g is observed with NBR copolymers over 35 percent ACN with the addition of LiBF_4 .

REFERENCES

1. J. Mocanin and E.F. Cuddihy, *J. Polym. Sci.* **14**, 313 (1966).
2. D.B. James, R.E. Wetton, and D.S. Brown, *ACS Polym. Prepr.* **19**, 347 (1978).
3. M. Watanabe and N. Ogata, in *Polymer Electrolyte Review* (J.R. McCullum and C.A. Vincent, eds.), pp. 52, Elsevier Applied Science, 1987).
4. R.E. Wetton, D.B. James, and W. Whitney, *J. Polym. Sci., Polym. Lett. Ed.* **14**, 577 (1976).
5. M. Watanabe, K. Nagota, M. Kanba, and I. Shinohara, *Polym. J.* **14**, 877 (1982).
6. A.K. Sircar and R.P. Chartoff, paper presented at the Symposium on Assignment of Glass Transition Temperature, Atlanta GA, March 3-4, 1993.
7. A.K. Sircar and T.G. Lamond, *Rubber Chem. Technol.* **51**, 647 (1978).
8. L.A. Chandler and E.A. Collins, *J. Appl. Polym. Sci.* **13**(8), 1585 (1969).
9. E.A. Collins, A-H. Jorgensen, and L.A. Chandler, *Rubber Chem. Technol.* **46**, 1087 (1973).
10. F.S. Cheng and J.L. Kardos, *Amer. Chem. Soc. Polymer Preprints*, 159th Meeting, p 615 (1969).
11. G. Williams, D.C. Watts, and J.P. Nottin, *J. Chem. Soc., Faraday Trans.* **1168**, 16 (1972).
12. W.H. Embree, J.H. Mitchell, and H.L. Williams, *Can. J. Chemistry* **29**, 253 (1951).
13. W. Hoffman, *Rubber Chem. Technol.* **37**, 1 (1964).
14. V.R. Landi, *Rubber Chem. Technol.* **45**, 222 (1972).

APPENDIX B

ANOMALY IN THE IONIC CONDUCTIVITY-TEMPERATURE STUDIES OF NBR COPOLYMERS USING DEA

INTRODUCTION

An acrylonitrile-butadiene copolymer (NBR) was chosen as the host polymer in the hybrid electrolyte study. It was expected that the lithium ion would coordinate with the nitrile group (CN) or NBR and thus promote ion transport. Commercial NBR copolymers contain 15 to 50 percent acrylonitrile. Therefore, it was necessary to screen the various acrylonitrile-butadiene copolymers with constant ratio of a lithium salt incorporated in the polymer with regard to their ionic conductivity. A TA Instruments DEA 2970 was used for this purpose.

A peculiar observation was a maximum between -25°C and $+25^{\circ}\text{C}$ in the conductivity-temperature curve which could not be attributed to any known phase-transition in the polymer. This is discussed in this study.

EXPERIMENTAL

Materials

The different NBR copolymers and their acrylonitrile (ACN) contents are shown in Table B-1. All NBR samples were supplied by Zeon Chemical Corp., Inc.

Films for dielectric analysis (DEA) were cast on the single surface electrode used by covering the electrode with a few drops of 3 percent solution of the polymer (with or without LiBF_4), either in DMF or NMP. The electrode containing the film was then dried inside a vacuum oven (500 mm mercury at room temperature), followed by high vacuum (75 mm mercury) at 80°C .

Dielectric Measurements

DEA 2970^[1] measures capacitance and conductance of a material as a function of time, temperature, and frequency. The instrument can operate between -150 to 500°C with the single surface electrode. The maximum limit for ionic conductivity measurement was found to be $10^{-3.5}$ at 100 KHz^[2]. The conductivity at 100 KHz is termed "apparent conductivity" and is close to the DC conductivity. The usefulness and limitations of DEA 2970 to measure ionic conductivity of polymeric electrolytes has been discussed before^[2]. A heating rate of $5^{\circ}\text{C}/\text{min}$ from -100 to $+125^{\circ}\text{C}$ under nitrogen purge was used for the present investigations. The samples were equilibrated at -100°C for 2 min before ramping.

Table B-1

NBR (or HNBR) Copolymers Used for the Study Versus Percent Bound ACN

Trade or Chemical Name	Bound ACN, %
Polyacrylonitrile	100
Nipol 1000X132	50.5
Nipol 1000X88	44.0
Nipol 1401LG	40.9
Nipol 1042	33.0
Nipol 1453HM	28.3
Nipol 1034-60	20.3
Nipol 1432 ^a	33.0
Zetpol 1020 ^b	44.0

^a Contains >20 percent vinyl acetate-vinyl chlorid copolymer (VYHH).^b Hydrogenated Nipol 1000X88, unsaturation 10%.

RESULTS AND DISCUSSION

Anomaly in the Conductivity-Temperature Curve

An example of the type of curves obtained for NBR copolymers is illustrated in Figure B-1 for HNBR (hydrogenated NBR with 44% ACN, Zetpol 1020). The glass transition temperature (T_g) for this copolymer is -22.8°C , determined at the extrapolated onset. It may be observed that the conductivity-temperature curve shows a maximum between -25 to $+25^\circ\text{C}$. The conductivity was expected to increase near T_g but its subsequent decrease at temperatures greater than T_g was unexpected.

Figure B-2 shows a selected portion of this curve in an amplified scale. After cooling and running the sample the next day, the intensity of the peak was lower and the peak position had shifted slightly to a higher temperature, but other characteristics were unaltered. It may be mentioned that Curve C refers to the unprogrammed cooling curve. Addition of an inorganic salt (LiBF_4) increased the conductivity in the whole range.

The same characteristics were observed for all NBR copolymers and at about the same temperature range. In contrast, T_g of NBR copolymers varies with nitrile content. This

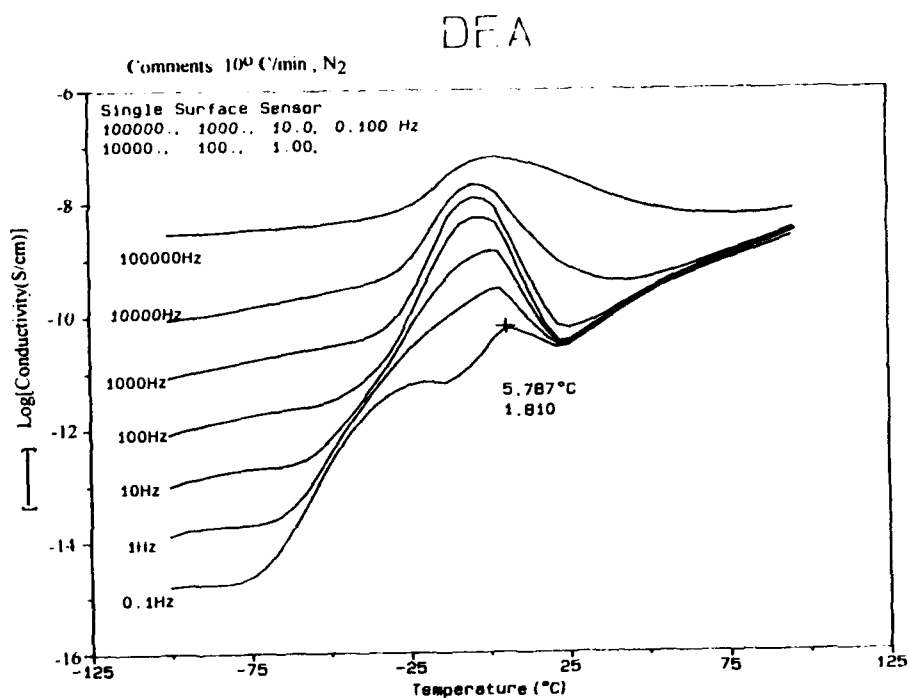


Figure B-1. DEA Curves of Hydrogenated HNBR (44% ACN, Zetpol 1020) Films Prepared from DMF Solutions.

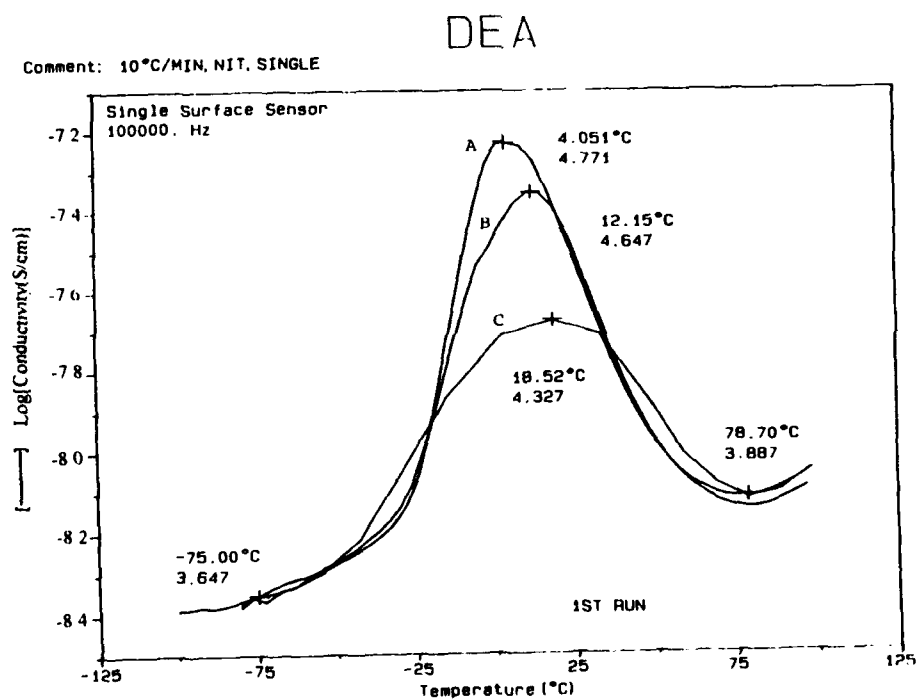


Figure B-2. Expanded DEA Curve of HNBR (44% ACN, Zetpol 1020). A=1st heat, B=2nd heat, C=cooling.

discounts any relationship of this peak with T_g . Unlike NBR (Figures B-2 and B-3), polyacrylonitrile (PAN) shows only slow increase of conductivity with temperatures without a maximum (Figure B-4). However, the incorporation of LiBF_4 (8:1) causes the maximum to appear (Figure B-5), although the peak height is much smaller and it is at a lower temperature than in NBRs.

Moisture Absorption

The fact that the addition of highly hygroscopic LiBF_4 in PAN causes the peak to appear at a location close to 0°C , suggests that absorbed or inadvertent admission of moisture may be responsible for the peak. However, when the specimens heated several times to 100°C are rerun, the same characteristics appear (Figures B-1, B-2, B-3, and B-5). This seems to preclude moisture, provided moisture can get in every time the sample inside the DEA assembly is cooled to low temperature before reheating.

Effect of Moisture in PEO

An experiment was conducted to investigate whether the anomalous peak would show in the presence of moisture in a film that does not normally show the above peak. Figures B-6 and B-7 represent the conductivity of polyethylene oxide (PEO) without moisture and equilibrated at 43 percent relative humidity for different periods. The small peak at -31.4°C may be attributed to T_g of PEO is at the frequency of the experiment (100,000 Hz). As expected, a slow increase of conductivity with temperature is observed after T_g . After the humidity treatment, the T_g peak moves to a slightly lower temperature, possibly due to plasticization by moisture, but a new peak is observed with a maximum around 10°C . This peak intensity decreases in the second high temperature run. Thus, moisture does give rise to an extra peak in the region where the anomalous peak for NBR is observed and behaves similarly to NBR in the first and second high temperature cycle, the latter having a smaller peak than the first. This experiment indicates that moisture may be responsible for the anomalous peaks. However, it may be noted that moisture was deliberately added to the PEO by treating it at 43 percent relative humidity for 36 hours, whereas the NBRs were kept in a dry dessicator. A query to the manufacturer revealed no other extraneous material except 2 to 3 percent (wt percent) of some oils and resins, used as an emulsifier. Interestingly, the DSC curve of many of the NBRs show small endotherm at around the -20 to $+20^\circ\text{C}$ range, as shown for an NBR with 28.5% ACN (Nipol 1453 MH), in Figure B-8. This is in the same temperature range as the anomalous ionic conductivity peak. However, the source of this endotherm is uncertain. Since the exact composition of the non-rubber components is proprietary information, it is not clear whether this could be attributed to the melting of the emulsifiers mentioned above.

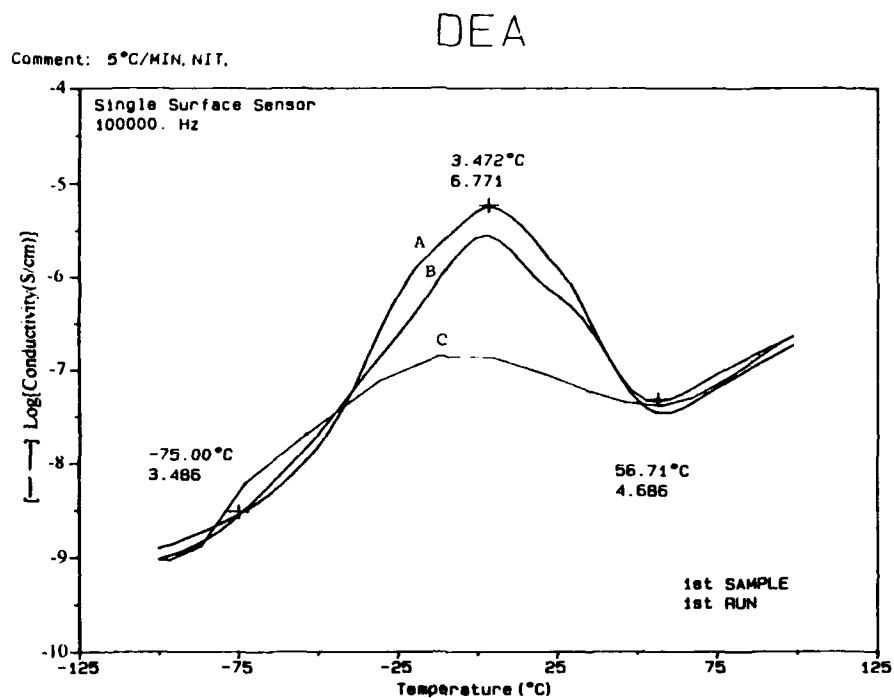


Figure B-3. Expanded DEA Curve of HNBR 44/LiBF₄ (CN/Li=8). A=1st heat, B=2nd heat, C=cooling.

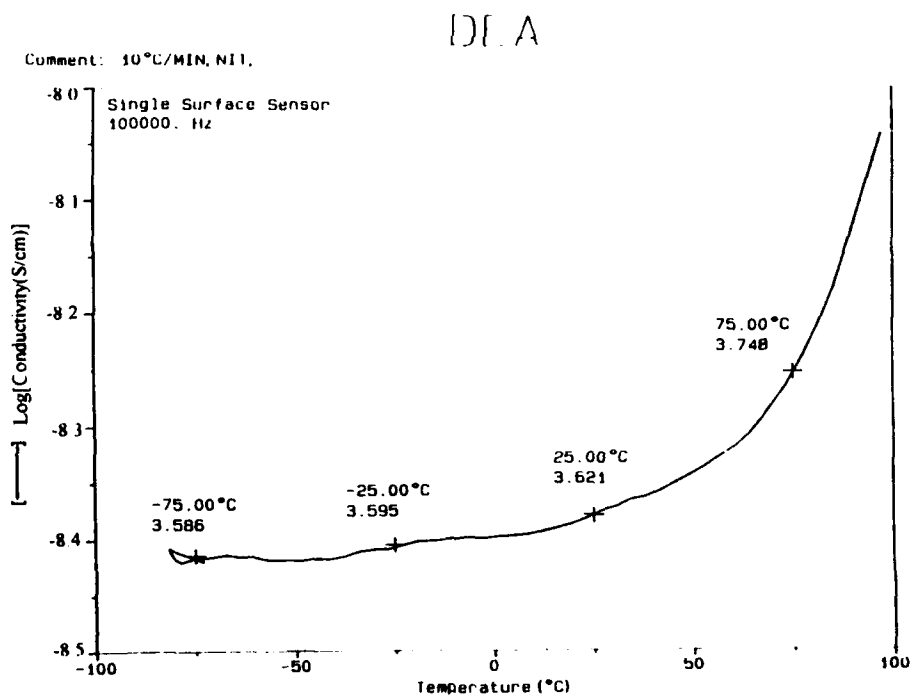


Figure B-4. DEA Curve of Polyacrylonitrile (PAN Dried from DMF).

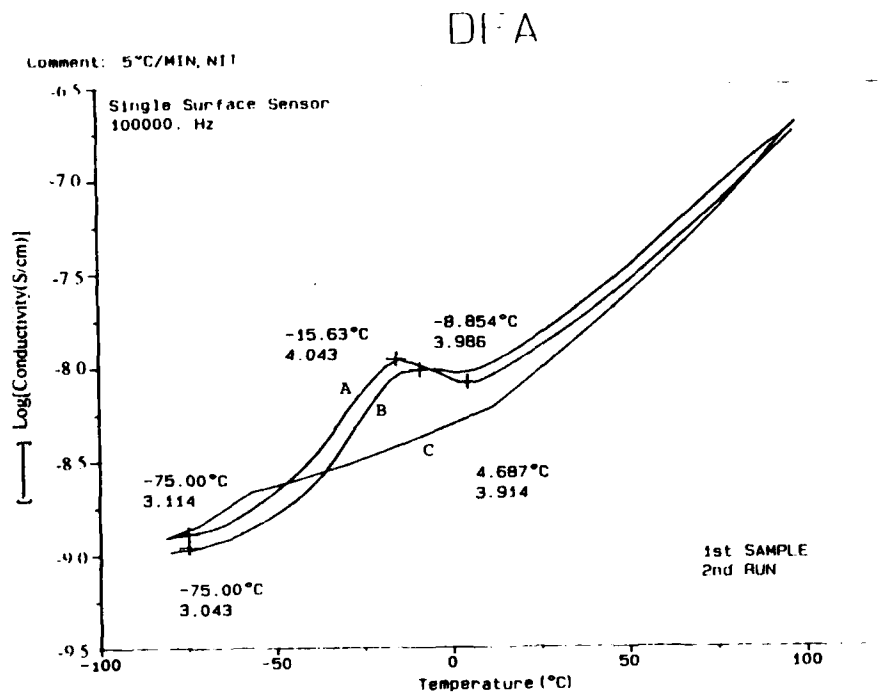


Figure B-5. DEA Curve of PAN/LiBF₄ (CN/Li=8). A=1st heat, B=2nd heat, C=cooling.

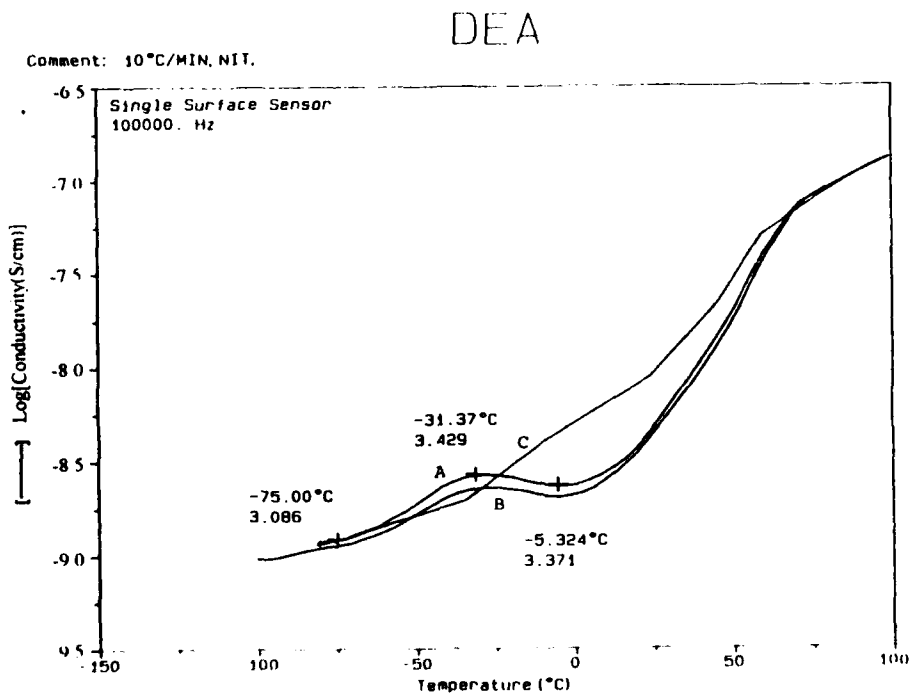


Figure B-6. DEA Curve for PEO.

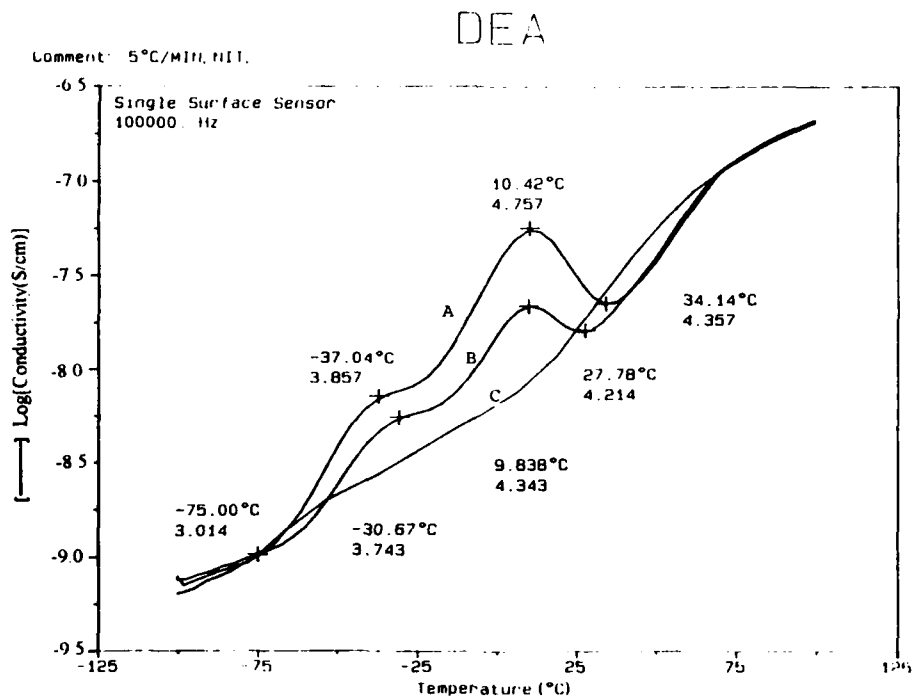


Figure B-7. DEA Curve for PEO After 68 Hours at 43% Relative Humidity.

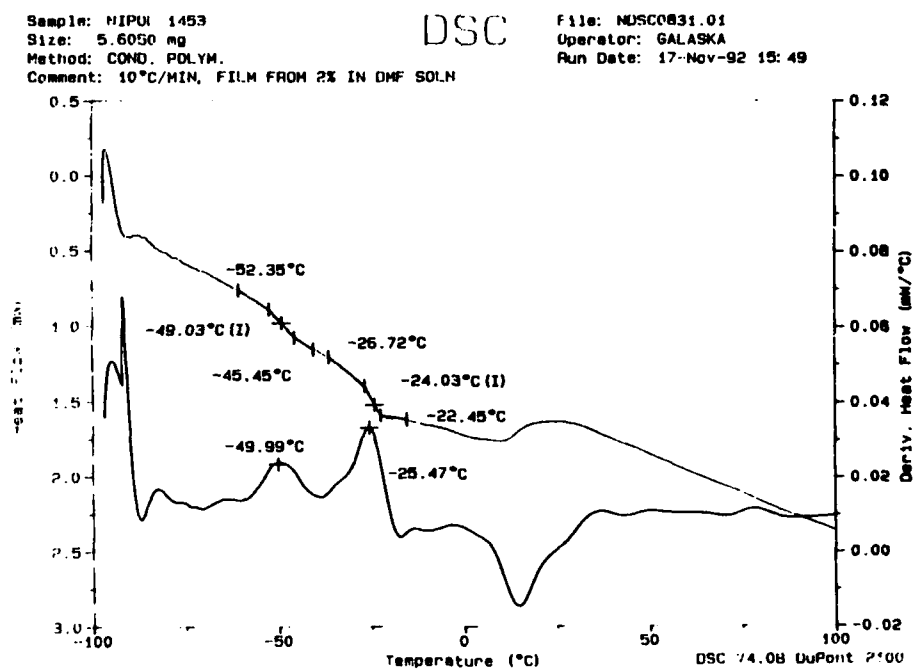


Figure B-8. T_g Determinant of NBR (28.3% ACN, Nipol 1453). Note the small endotherm after the T_g Region.

Literature Search

A literature search reveal no clue to the above anomaly. Petrea et al.^[4] observed a maximum in the dielectric constant versus time curve of cured NBR rubbers, ascribed to the extra mobility of the molecular chains due to plasticization by other ingredients. However, this was absent in pure rubbers.

Effect of Plasticizers

It was observed that the above maximum is not observed either in PAN (Figure B-9) or hydrogenated NBR (Figure B-10) when the system includes a plasticizer (e.g., DMAC or EC). This may be ascribed to the fact that ionic conductivity is being higher by several orders of magnitude which masks any variation of small background ionic phenomenon. Thus, the above anomaly would not seriously restrict the use of NBR polymers as host material for hybrid electrolytes.

Ionic Conductivity of Different NBR Copolymers

The primary reason for using DEA 2970 to measure ionic conductivity of NBR copolymers was to have a quick scan of different copolymers to select one with the highest conductivity. In view of the conductivity maximum mentioned above, it was very difficult to compare ionic conductivity of different NBRs. Table B-2 presents a summary of the conductivity data between -75 to +75°C at an interval of 25°C. The data do not show a definite trend. Conductivity is also influenced by the solubility of the sample, as in the case of 1000X132 which has the highest ACN content (50:5 percent) but is sparingly soluble in DMF. It has lower conductivity than 1000X88 which has lower ACN content (44 percent). If Nipol 1000X132 is excluded from Table B-2, Nipol 1000X88, which has the highest ACN, would also have the highest overall conductivity. However, the trend is not clear and the conductivity difference is small. This indicates the possibility of some participation of the double bond in promoting conductivity. Migahed et al.^[5] observed higher DC conductivity for NBR (28) than those for NBR (38) and PAN. They suggested that electronic conductivity of NBR originates from π -electrons in the conjugated double bond systems and carried by electron hopping model. However, no indication of coupling Li^+ with the double bond is observed from IR data in the present study.

CONCLUSIONS

No definite clue as to why the anomaly occurs could be found. However, there are some indications that the anomaly may be related to absorption of moisture. These indications are summarized as follows.

1. The maximum of conductivity occurs between -25 to +25°C with a peak around 0°C.
2. The addition of LiBF₄ (which is highly hygroscopic) to PAN makes the peak appear where as pure PAN does not show the peak.
3. Treating PEO at 43 percent relative humidity makes the peak appear. Pure PEO does not show this peak.

However, these are all circumstantial evidences. The fact that the same peak appears in the second or third cycle after heating the electrode with the sample to 175°C is an argument against moisture being responsible for the peak. Thus, no definite conclusion can be reached at this time as to the reason for this anomalous peak.

REFERENCES

1. T.A. Instruments Literature on DEA 2970.
2. A.K. Sircar, P.T. Weissman, B. Kumar, and R.A. Marsh, *Thermochim Acta* (In Press).
3. L.A. Chandler and E.A. Collins, *J. Appl. Polym. Sci.* **13**, 1585 (1969).
4. I.C. Petrea, C.A. Stansen, M. Gojagaru and E. Barna Analele, *Univ. Bucuresti Fizica* **29**, 57 (1980).
5. M.D. Migahed, A. Tawausi, and N.A. Bahr, *Eur. Polym. J.* **18**, 975 (1982).

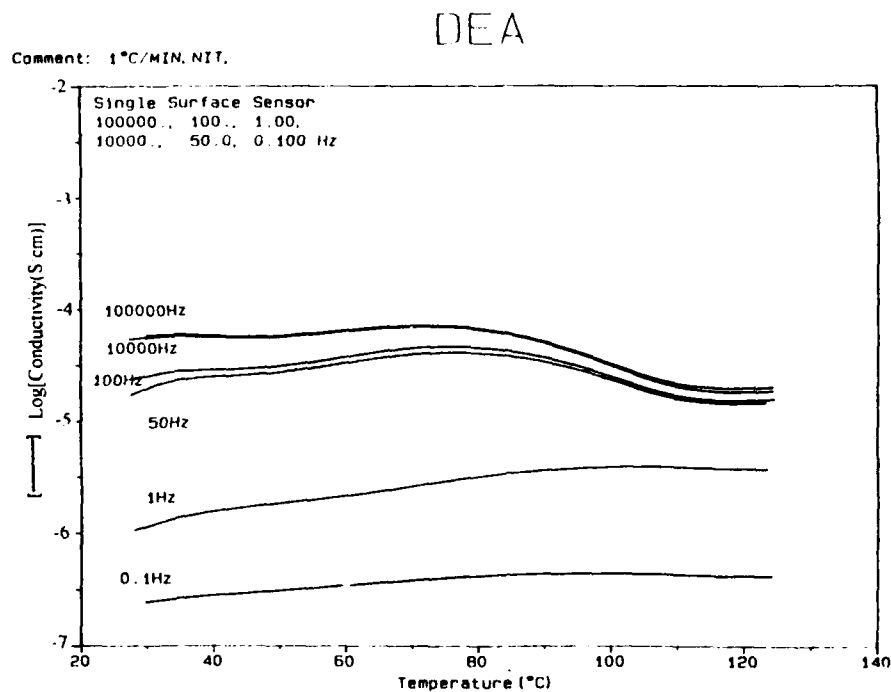


Figure B-9. DEA Curve of PAN/LiBF₄/EC (CN/Li=4, 25% EC).

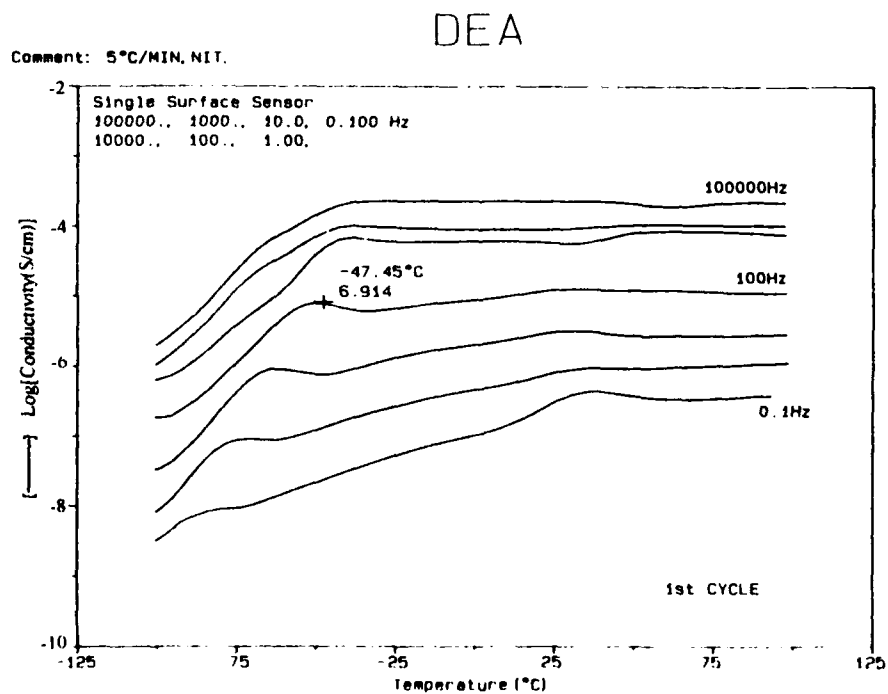


Figure B-10. DEA Curve of Zetpol 1020/LiBF₄/DMAC (CN/Li=8, 75% DMAC) Gel.

TABLE B-2
Conductivity of NBR and HNBR Elastomers with LiBF₄ (CN:Li=8)
at Different Temperatures at 10⁵ Hz

Sample ID CN:Li 8:1	Conductivity (mhos/cm x 10 ⁹)				
	-75°C	-25°C	0°C	25°C	75°C
PAN	1.3	20.0	200.0	31.6	31.6
Nipol-1000X132 (50.5% ACN)	3.2	15.8	79.4	25.1	31.6
Nipol-1000X88 (43.9% ACN)	1.0	100.0	316.0	50.1	79.4
Nipol-1401LG (40.9% ACN)	1.0	2.5	20.0	15.8	12.6
Nipol-1432 (33.2% ACN)	1.3	6.3	15.8	12.6	6.3
Nipol-1034-60 (21.3% ACN)	3.2	7.9	50.1	7.9	20.0
Zetpol-1020 (44.5% ACN)	2.0	31.6	631.0	63.1	39.8